

# Integrated Analysis of the Transcriptome and Metabolomics Reveals an Essential Role for Auxin in Hypocotyl Elongation During End-of-Day Far-Red Treatment of *Cucurbita Moschata*

**Qi Liu**

Northwest Agriculture and Forestry University

**Hanqing Zhang**

Northwest A&F University: Northwest Agriculture and Forestry University

**Yanhao Mei**

Northwest A&F University: Northwest Agriculture and Forestry University

**Qi Li**

Northwest A&F University: Northwest Agriculture and Forestry University

**Yahui Bai**

Northwest A&F University: Northwest Agriculture and Forestry University

**Huibin Yu**

Northwest A&F University: Northwest Agriculture and Forestry University

**Xiaodong Xu**

Northwest A&F University: Northwest Agriculture and Forestry University

**Jianxiang Ma**

Northwest A&F University: Northwest Agriculture and Forestry University

**Yongjun Wu**

Northwest A&F University: Northwest Agriculture and Forestry University

**Zhenchao Yang** (✉ [yangzhenchao@126.com](mailto:yangzhenchao@126.com))

Northwest A&F University: Northwest Agriculture and Forestry University <https://orcid.org/0000-0002-0017-4348>

---

## Research article

**Keywords:** *Cucurbita moschata*, far-red light, auxin, transcriptome, metabolomics

**Posted Date:** December 2nd, 2020

**DOI:** <https://doi.org/10.21203/rs.3.rs-113698/v1>

**License:**  This work is licensed under a Creative Commons Attribution 4.0 International License.

[Read Full License](#)

---

# Abstract

## Background

Long, robust hypocotyls are important for facilitating greenhouse transplant production. Use of far-red light at the end of the day (end-of-day far-red, EOD-FR) is known to affect hypocotyl elongation. Auxin is an important regulator of plant growth and development, but its role and mechanism in EOD-FR-mediated hypocotyl elongation remain unclear. Here we combined transcriptome sequencing and metabolite profiling of pumpkin hypocotyls with related physiological experiments to provide insight into the mechanisms by which auxin affects the response to EOD-FR.

## Results

After EOD-FR treatment, the length of pumpkin Hypocotyl and the IAA level of plant Hypocotyl were significantly promoted. When NPA was applied, the Hypocotyl elongation mediated by EOD-FR and the increase of IAA content were counteracted.

At the same time, through the observation of Hypocotyl sections, we found that hypocotyl cells expanded significantly after EOD-FR treatment. After EOD-FR treatment, 2801 DEGs, were identified in hypocotyl, of which 31 DEGs related to auxin synthesis, transport and signal transduction and 25 cell wall protein genes were identified. Through the detection of metabolic group, it was found that the levels of tryptophan and indole in plant increased after EOD-FR treatment. All these indicate that auxin plays an essential role in EOD-FR-mediated hypocotyl elongation.

## Conclusions

We identified a large number of differentially expressed genes related to auxin synthesis, transport, and downstream response. We speculate that auxin is essential for pumpkin hypocotyl elongation mediated by EOD-FR, and that the synthesis of free IAA may be performed by the tryptophan-dependent TAA-YUC pathway. This study improves our understanding of auxin's role in EOD-FR-mediated hypocotyl elongation.

# Background

The control of plant morphology is critical to commercial greenhouse transplant production [1]. As an important transplant production technique, grafting plays a key role in controlling soil-borne diseases and improving plant resistance to abiotic stress during crop cultivation [2]. In vegetable grafting propagation, the use of rootstocks with long hypocotyls and uniform growth can improve grafting speed and prevent vulnerable scions from coming into contact with the soil during and after transplant [1]. However, because seasonal variation in greenhouse environmental conditions affects elongation, the continuous production of rootstocks with long and uniform hypocotyls remains a significant challenge [3].

Light is essential for plant growth and development, serving as an energy source for photosynthesis and an environmental cue for photomorphogenesis [4]. Numerous studies have confirmed that the use of different light quality treatments significantly affects early plant morphology, specifically the promotion of seedling hypocotyl elongation [5, 6][4, 5]. In recent years, artificial light sources have become a new type of ‘intelligent’ equipment in agricultural production facilities, particularly for vegetable production [7]. Based on the production goals and crop light demand, optimum light conditions for crop growth can be provided. New opportunities for the production of long hypocotyl rootstocks in growth facilities are now possible.

The use of far-red light at the end of the day to affect plant hypocotyl length has been studied by biologists for many years [1, 3, 8, 9]. The technique is based on plants’ use of phytochrome to sense the red/far-red ratio (R/FR) of the external light environment [10]. When FR light is absorbed, the structure of phytochrome changes reversibly from active Pfr to Pr [11]. Decreased Pfr content in the nucleus leads to an increase in the activity of phytochrome interacting factors (PIFs) [12]. In this way, phytochrome perceives information on the surrounding light and correspondingly mediates the expression level of genes regulated by PIF [13]. EOD-FR can mimic growth in low R:FR conditions by decreasing Pfr levels before the onset of darkness, thereby maintaining a low Pfr throughout the dark period [14].

Previous studies have shown that EOD-FR mediates the hypocotyl elongation of tomato, pumpkin and other crops without affecting plant dry weight, stem diameter, or seedling index. There is flexibility in the selection of FR light intensity and duration to provide a sufficient FR light dose (light intensity × duration). When the dose of FR light falls within a certain range, the response of hypocotyl length can be described accurately by the Michaelis–Menten saturation curve [3]. Therefore, EOD-FR has significant potential for the morphological regulation of seedlings in growth facilities [1, 3].

Although research on EOD-FR is continuously being performed, there have been few studies on the mechanisms by which EOD-FR promotes hypocotyl elongation. A variety of phytohormones are known to regulate elongation growth in response to the R:FR environment [13, 15]. Among them, auxin is thought to be one of the most important factor [16, 17], but its specific role in EOD-FR-induced elongation has not been studied in detail. Moreover, although researchers have previously used RNA-seq to analyze differences in the transcriptome of *Platycodon grandiflorum* after EOD-FR treatment [18], the auxin signaling pathway is extremely complex, and there are many auxin response genes in a single family. The complexities of auxin response involve the modulation of both transcriptional and metabolic networks, and the use of RNA-seq alone has limitations in predicting the central metabolic pathways and pivotal reactions that underlie this phenomenon [19].

In recent years, the use of metabolomics techniques for the quantitative analysis of small molecular weight plant metabolites has become increasingly widespread. These techniques enable researchers to explore the relationships between metabolite levels and phenotypic changes, providing new insights into multiple phenomena [20].

Pumpkin, the vegetable of Cucurbitaceae, has stronger root system, disease resistance and stress resistance, so it is widely used as rootstock in the grafting of melons [21]. Here, we performed metabolite and transcriptional profiling of pumpkin (*Cucurbita moschata*) hypocotyls exposed to EOD-FR and combined these results with related physiological measurements to investigate the role of auxin in EOD-FR-mediated hypocotyl elongation and identify key genes and pathways. The expression of a subset of genes was verified by quantitative real-time polymerase chain reaction (qRT-PCR). The resulting data expand our understanding of auxin synthesis and signal transduction during EOD-FR-mediated elongation at the metabolic and molecular levels. They also provide valuable mechanistic information for the application of EOD-FR in greenhouse production settings.

## Results

### Effects of EOD-FR light on growth and hypocotyl cell morphology of pumpkin seedlings

Hypocotyls were significantly longer in EOD-FR-treated plants than in control plants (Fig. 1a). However, there were no significant differences in stem diameter or above- and belowground fresh and dry weights between the CK and T. After treatment with inhibitors, not only was hypocotyl elongation inhibited, but stem diameter and dry and fresh weights also decreased significantly (Fig. 1b). Using axial sections of hypocotyl cells (Fig. 2a), we observed the length and width of parenchyma cells in the four treatments (Fig. 2b). Result showed hypocotyl parenchyma cells expanded significantly after EOD-FR treatment.

### Changes in auxin level after EOD-FR treatment

To further explore the role of auxin in EOD-FR-mediated hypocotyl elongation and cell expansion, we measured IAA in leaves and hypocotyls from the different treatments. With LC-MS, we found that the level of free IAA in hypocotyls of the EOD-FR seedlings was significantly higher than that of other treatments (Fig. 3). Treatment with the auxin transport inhibitor NPA eliminated the increase in free IAA induced by EOD-FR. The IAA content in leaves increased significantly after EOD-FR treatment, and the content of IAA in leaves of the NPA-T group was the highest. When NPA was applied alone, the IAA content of leaves and hypocotyls decreased significantly. The above results indicate that EOD-FR treatment can increase free IAA levels in the plant, especially in the hypocotyl, but that this effect is counteracted by NPA. This shows that the level of free IAA in the hypocotyl is an important factor in promoting cell expansion and hypocotyl elongation.

### Metabolomics analyses and identification of differentially abundant metabolites

To investigate the source of free IAA synthesis in hypocotyls under EOD-FR, we analyzed their metabolic profiles using LC-MS/MS. A principal component analysis (PCA) model was constructed (Additional file 7) to study the relationships between metabolite levels and EOD-FR by R (Used package including vegan, stats and ggplot2). Based on PCA analysis of metabolites identified in the positive and negative ion modes, we found that metabolite accumulation in the hypocotyls was quite different between CK and T.

We specifically identified metabolites (Additional file 1) related to auxin synthesis. Compared with the CK, EOD-FR plants accumulated more tryptophan and indole: their abundances increased 2.14-fold and 2.05-fold, respectively. Tryptophan is an important precursor for auxin-IAA, and indole is a precursor for tryptophan [22]. In addition, the content of 3-indole acrylic acid (IAcA), another product of the tryptophan metabolic pathway, also increased significantly after EOD-FR treatment.

We compared the correlation coefficients of tryptophan, indole, and IAA metabolites measured above, and found that the correlations between them were greater than 0.9 (Additional file 8), it strongly suggesting that newly produced free IAA was synthesized by a tryptophan-dependent IAA synthesis pathway.

## RNA-seq analysis

Transcriptome profile comparisons were performed with the same experimental materials used for metabolic profiling. The sizes of the sequenced libraries ranged from 40,704,360–54,037,758 bp (Additional file 2), and the Q30 percentage (percentage of sequences with an error rate <0.1%) was over 93% for each library. A total of 44.19 G of raw sequencing data was generated, and 32,205 expressed unigenes were identified. Overall, the RNA-seq data were of high quality and could be used for further analysis.

### Identification of DEGs in hypocotyls after EOD-FR treatment

DEGs analysis indicated that 1968 genes were upregulated and 833 genes were downregulated in hypocotyls after EOD-FR treatment (Additional file 3, Additional file 9 and Additional file 10). GO enrichment analysis of upregulated genes (Additional file 4 and Additional file 11) demonstrated that GO terms related to cell division and cell wall metabolism were significantly enriched. Terms such as cell wall biogenesis, plant-type cell wall, cell wall, cell population proliferation, xyloglucan metabolic process, xyloglucan:xyloglucosyl transferase activity, and plant-type secondary cell wall biogenesis were among the top 20 enriched terms.

The metabolic pathways associated with the DEGs were explored further by KEGG enrichment analysis. The KEGG enrichment scatterplot showed that starch and sucrose metabolism (K00500) and amino sugar and nucleotide sugar metabolism (K00520) were the two pathways with the highest degree of enrichment. Sixty-four and 44 genes were involved in these two significantly enriched pathways, respectively (Additional file 5 and Additional file 11).

### Identification of key cell wall protein genes associated with cell expansion

Plant growth is inseparable from cell expansion and division, a fact that is confirmed by the morphological changes in hypocotyl cells and the transcriptome results documented here. Likewise, the expansion of plant cells is inseparable from the regulation of various cell wall modification proteins [23]. Expansins (EXPs) and endotransglucosylase/hydrolases (XTHs) play an crucial role in the regulation of cell wall relaxation and remodeling [24, 25]. Therefore, we identified these two critical cell wall modification proteins from the transcriptome data and examined their expression. Twelve EXP homologs

and 13 *XTH*/homologs were identified based on BLAST results from the NCBI NR database (Fig. 4), and their expression was significantly upregulated after EOD-FR treatment. Therefore, EOD-FR appears to stimulate the activities of XTHs and EXPs, which are important for cell expansion and hypocotyl elongation.

### Identification of auxin-related DEGs

Auxin has been shown to play key roles in the promotion of hypocotyl elongation in low R:FR environments. Therefore, we identified DEGs related to auxin synthesis and auxin signaling pathways using the GO, KEGG, and NR databases.

We identified a total of 31 auxin-related genes, including three key genes in the TAA-YUC (IPyA) plant auxin biosynthesis pathway: a tryptophan aminotransferase-related protein 2 (TAR2) homolog and two indole-3-pyruvate monooxygenase (YUCCA) homologs. Their expression was significantly increased 2.24-, 2.36-, and 3.49-fold after EOD-FR treatment, respectively. In addition, a N-(5-phosphate ribose) o-aminobenzoate isomerase 1 gene, which encodes a key enzyme in tryptophan biosynthesis by the shikimic acid pathway, was also significantly upregulated.

We also identified 14 DEGs encoded auxin-responsive proteins, including four AUX/IAAs, six SAURs, one ABP1, one GH3, and one LIR1, ten auxin transporter-like genes, including genes encoding six influx carriers (AUX-LIKE), two efflux carriers (PIN and PIN-LIKE), two ATP-binding cassette transporters (ABCB) and one WALLS ARE THIN 1 (WAT1) transporter. Finally, we identified two genes that indirectly affect auxin levels; these two CBL-interacting serine/threonine protein kinase related genes were also upregulated under EOD-FR treatment. The expression levels of these genes are presented in the form of a heatmap (Fig. 5).

### Integrated analysis of the transcriptome and metabolomics

We calculated Pearson correlation coefficients of indole, tryptophan, and IAA with auxin direct-related genes and drew a corresponding heatmap (Fig. 6). Seventeen genes had correlation coefficients greater than 0.8 with tryptophan, and 10 of these genes had correlation coefficients greater than 0.9. Six genes had correlation coefficients greater than 0.8 with indole, and three had correlation coefficients greater than 0.9. Fifteen genes had correlation coefficients greater than 0.8 with IAA, and four had correlation coefficients greater than 0.9. The correlations of CmoCh19G001500 (YUCC8, a key enzymes in auxin synthesis), CmoCh06G001560 (endoplasmic reticulum transporter PIN-LIKES 5), CmoCh19G007280 (auxin-induced protein 15A), and CmoCh07G008650 (IAA-amino acid hydrolase ILR1-like 3) with the three metabolites were more than 0.8. Finally, based on the reported auxin regulatory network in *Arabidopsis* and other plants, we proposed a hypothetical pathway by which auxin regulates pumpkin hypocotyl elongation under EOD-FR (Fig. 7).

### qRT-PCR

qRT-PCR was used to validate the RNA-seq transcriptomic data. We selected six DEGs for qRT-PCR verification (Additional file 12), and their relative expression measured with qRT-PCR was consistent with their FPKM values in the RNA-seq dataset ( $R^2 = 0.8607$ ,  $P < 0.01$ ) (Additional file 13), indicating that the RNA-seq data were reliable for further analysis. To verify the effect of auxin on gene expression, we selected eight auxin-related genes and measured their expression in the CK, T, NPA-T, and NPA-CK treatments with qRT-PCR, as shown in Fig. 8. After NPA treatment, the expression of the eight genes decreased significantly. All the primers designed are listed in Table S3.

## Discussion

Emerging evidence indicates that auxin plays an important role in the regulation of plant elongation in a low R:FR environment. However, the specific mechanisms by which auxin mediates hypocotyl elongation in response to EOD-FR are uncertain. Previous studies found that (1) EOD-FR treatment significantly increased seedling hypocotyl elongation but had no effect on stem diameter, biomass, or seedling index [1, 3], and (2) that the immediate cause of hypocotyl elongation was the expansion of hypocotyl cells [18]. The results of the present experiment confirm these conclusions.

We found that the polar auxin transport (PAT) inhibitor NPA completely abolished EOD-FR-induced elongation and caused significant decreases in stem diameter, dry weight, fresh weight, and hypocotyl IAA content. It is worth mentioning that the level of IAA in NPA-T leaves was significantly higher than that of other treatments. We speculate that EOD-FR treatment increased leaf IAA levels, but this IAA could not be transported to the hypocotyl by PAT and therefore accumulated in the leaves. The increase of free IAA content in hypocotyls after EOD-FR treatment therefore appears to be closely related to PAT activity.

Next, we performed a detailed investigation of the mechanisms by which auxin affects hypocotyl elongation under EOD-FR, using a combination of transcriptome profiling, metabolomics analysis, and physiological measurements.

### Auxin is essential for EOD-FR-mediated hypocotyl elongation

As early as 2008, Csukasi et al. had discovered TAA1, a key enzyme in the first step of auxin biosynthesis under low R:FR conditions [16]. Since then, increasing numbers of researchers have performed in-depth studies to demonstrate that auxin plays a vital role in low-R:FR-mediated elongation. However, EOD-FR is a special form of far-red light treatment, and few studies have addressed its relationship to auxin. Here, we have shown that auxin is essential for EOD-FR-mediated hypocotyl elongation. Several lines of evidence support this conclusion.

First, after EOD-FR treatment, the level of free IAA in hypocotyls increased significantly during EOD-FR treatment. However, hypocotyl elongation mediated by EOD-FR was abolished in the presence of the PAT inhibitor NPA. Second, we identified a large number of DEGs related to auxin biosynthesis, transport, and response in EOD-FR-treated plants (Fig. 5). Third, the content of tryptophan, a key auxin synthesis precursor, increased significantly after EOD-FR treatment (Additional file 1). Taken together, these results

strongly suggest that auxin plays an essential role in the regulation of hypocotyl elongation in response to EOD-FR.

### The pathway of auxin biosynthesis after EOD-FR treatment

There are multiple auxin biosynthetic pathways in plants, and the TAA-YUC pathway (IPyA pathway) appears to be the primary pathway that responds to low R:FR [16]. TAA1 catalyzes the first step in this pathway [26], and a family of enzymes encoded by YUCCA genes catalyze the second step [27]. YUCCA appears to mediate the rate-limiting step in IAA synthesis [28, 29].

RNA-seq data showed that the expression of one TAA1-related TRYPTOPHAN AMINOTRANSFERASE RELATED 2 (TAR2) gene and two YUCCA genes were upregulated under EOD-FR. Here, we found a significant correlation between YUCC8 expression levels and the abundance of three auxin-related metabolites and previous studies have shown that YUCC8 is closely related to the response of plants to dark environments and that its expression increases significantly in low R:FR environments [30]. Therefore, YUCC8 may be a key gene that specifically responds to EOD-FR. All of these results indicate that the TAA-YUC pathway is the main route for free IAA synthesis in response to EOD-FR treatment.

Increased L-tryptophan content in hypocotyls under EOD-FR also confirms the above conjecture[16]. Tryptophan is an important precursor of auxin synthesis, and its content is closely related to the level of plant auxin. It has previously been shown that IAA levels in rice calli and potato buds with excessive tryptophan synthesis increased 57- and 39-fold, respectively [31, 32].

Moreover, the expression of a gene encoding N-(5'-phosphoribosyl) anthranilate isomerase 1 (trpF) in the tryptophan synthesis pathway and the abundance of the tryptophan precursor indole [22] also increased significantly after EOD-FR treatment. These may be important mechanisms underlying the increased tryptophan observed in plants under EOD-FR. The trpF appears to be a key gene of tryptophan metabolism induced by EOD-FR.

### Auxin transport is enhanced by EOD-FR treatment

Based on changes in plant morphology and auxin levels after NPA treatment, we believe that PAT is necessary for hypocotyl elongation mediated by EOD-FR. PAT is accomplished through the concerted action of PIN-FORMED (PIN) efflux carriers, P-GLYCOPROTEIN/ATP-BINDING CASSETTE B4 (PGP/ABCB) family members, and auxin influx AUXIN1/LIKEAUXIN1 (AUX/LAX) transporters, all are important for increasing IAA transport to specific cell types [33].

Polarly distributed PINs have been shown to play an important role in plant elongation and growth under low R:FR [34]. Here, we found that the expression of PIN4-related genes was significantly upregulated after EOD-FR treatment, consistent with the findings of Takemura et al in a study of *Platycodon grandiflorum* [18]. PIN4 may therefore be a crucial efflux carrier protein for EOD-FR-mediated elongation.

In addition, a gene encoding PIN-like (PILS) protein, which is structurally similar to PIN, was also identified in our transcriptome data. PILS localizes to the endoplasmic reticulum and participates in the dynamic balance of auxin in that organelle [35]. We found that the expression of PILS5 was significantly downregulated 7.7-fold in response to EOD-FR. Decreased PILS5 expression seems to suggest a cumulative decrease in IAA in the ER, causing more IAA to flow into the nucleus and influence various biological processes [36], but further studies are needed to identify specific underlying mechanisms.

Unlike PINs, ABCB proteins are involved in the ATP-dependent influx and efflux of auxin and are located uniformly throughout the plasma membrane [37]. In the *sav4* mutant with a basic auxin transport deficiency, auxin efflux mediated by ABCB is blocked, and the plant's ability to respond to low R:FR is significantly impaired [38], indicating that ABCB is necessary for the low R:FR response. Here, two genes encoding proteins similar to ABC transporter B family member 19 (ABCB19) were significantly upregulated under EOD-FR. It has been reported that ABCB19 can affect the elongation of hypocotyls [39] and stabilize PIN proteins on the plasma membrane to coordinate the regulation of auxin efflux [40]. In addition to auxin efflux carriers, AUX1-LIKE (LAX) auxin influx carriers were also significantly upregulated after EOD-FR treatment. Studies on AUX/LAX in other plants have shown that hypocotyl length is significantly reduced in the *PaLAX1* mutant compared to that of wild type [41], and there is a close relationship between PIN and LAX [42]. At present, there are few studies of AUX/LAX genes under low R:FR conditions, but it is likely that they play an indispensable role in EOD-FR-mediated hypocotyl elongation. Here, we identified six *LAX*-like genes that may have a role in the EOD-FR response (Fig. 5). We also identified a gene related to vacuolar auxin transport, WALLS ARE THIN 1 (WAT1), whose encoded protein is involved in maintaining the dynamic balance of intracellular auxin [43].

In addition to carriers that directly participate in auxin transport, two CBL-interacting serine/threonine protein kinase (CIPK) related genes were significantly up-regulated after EOD-FR treatment. CIPKs can participate in auxin transport by regulating gene expression; for example, the tobacco high-expression CIPK mutant CaCIPK6T1878-90 shows increased basic auxin transport [44].

Here, we showed that many genes related to auxin transport are significantly upregulated after EOD-FR treatment; this may enhance the transport of free auxin to the hypocotyl, thereby increasing its IAA level. Synergy among various auxin transport carriers is probably required to maintain the auxin concentrations necessary for regulation of plant growth and hypocotyl elongation in response to EOD-FR. At present, the specific functions of these DEGs remain to be studied in pumpkin.

### **EOD-FR significantly affects the component of auxin signal transduction in hypocotyl cells**

The cellular response associated with free auxin was transduced through a specific signal transduction pathway [45]. In the nucleus, auxin regulates the expression of downstream genes by specifically activating auxin response factors (ARFs) through the SCFTIR1/AFB-AUX/IAA pathway [46], in turn regulating the expression of downstream genes. It has been reported that the *AUX/IAA*, *GH3*, and *SAUR* gene families are the main downstream response genes induced by auxin in the nucleus [47], and low-R:FR-mediated elongation is closely related to their expression in *Arabidopsis* [48, 49].

Relevant studies have shown that the stability of AUX/IAA proteins is enhanced in the *PhyA* mutant, weakening the low-R:FR-mediated elongation reaction [50]. Furthermore, the expression of AUX22 is significantly lower in auxin-insensitive mutants than in wild-type plants under low R:FR conditions [51]. Here, we identified four AUX/IAA genes (Fig. 5), including two AUX22 genes, suggesting that AUX22 may affect hypocotyl elongation in response to EOD-FR treatment. Two AUX/IAA genes (IAA11 and IAA14) were also significantly up-regulated and may be important candidate genes in the EOD-FR response.

The GH3 gene family is related to the formation of auxin conjugates and regulates plant auxin homeostasis. Hypocotyls of *Arabidopsis* with GH3.17 deficiency accumulated more IAA and exhibited increased sensitivity to a low R:FR environment, resulting in longer hypocotyls [17]. In our study, the expression of GH3.6 decreased significantly 9.35-fold after EOD-FR treatment. Recent research shows that overexpression of GH3.6 in the *Arabidopsis* mutant *dwarf in light 1-D* (*df1-D*) produces strong developmental phenotypes such as short hypocotyls [52]. Here, up-regulation of ILR1 and down-regulation of GH3.6 suggest that the mechanisms underlying increased free IAA in hypocotyls under EOD-FR treatment are complex, although the regulation of IAA homeostasis clearly plays a certain role.

In recent years, SAURs have been shown to play an important role in the auxin-related regulation of apoplast acidification [53]. Specifically, SAUR proteins inhibit the activity of phosphatases, thereby preventing plasma membrane H<sup>+</sup>ATPase dephosphorylation and activating H<sup>+</sup>ATPases, which in turn leads to apoplast acidification and the promotion of cell wall protein activity [54]. We found that several SAUR genes were significantly up-regulated after EOD-FR treatment (Fig. 5). SAUR71 has been shown to regulate hypocotyl stele growth in *Arabidopsis* [55], and SAUR50 has been shown to promote hypocotyl elongation in the dark [56]. The increased expression of SAUR genes likely contributed to apoplast acidification in hypocotyl cells after EOD-FR treatment, in turn affecting plant growth. At present, the functions of many SAUR proteins remain unknown, but as the largest family of auxin early response genes, SAURs are undoubtedly very important for EOD-FR-mediated hypocotyl elongation.

In addition to the typical nuclear auxin signal transduction pathway, some auxin-regulated processes are controlled by the independent TIR1/AFB-AUX/IAA pathway [57]. The related molecular basis has not yet been clarified, but auxin binding protein 1 (ABP1) is involved in some of these processes [57, 58]. In response to low R:FR, the expression levels of several genes regulated by auxin and shading in *abp1-5* mutants were 3–5 times lower than those in the Col wild type, indicating that ABP1 is also an important factor in FR response [59]. We found that the expression of auxin receptor abp19a-related genes increased significantly after EOD-FR treatment. Although many studies have shown that ABP1 has an important role in plant growth, more in-depth studies are needed to analyze its role in the EOD-FR response. In summary, after EOD-FR treatment, there were significant differences in the expression of different auxin response genes in cells, which presumably led to physiological phenomena such as cell expansion.

## EOD-FR treatment enhances the activity of cell wall proteins

Hypocotyl elongation induced by EOD-FR is closely related to cell wall relaxation and activity. In this process, cell wall proteins play an important role in cell expansion [23]. Research shows that XTHs act on xylan chains, relax the cell wall, accelerate cell wall remodeling, and regulate cell expansion [60]. EXPs cause wallloosening by disrupting non-covalent interactions between cellulose microfibrils and matrix polysaccharides [61].

Previous studies have shown that the expression levels of XTH22 in the *doc1/BigArabidopsis* mutant are significantly lower than those in the wild type under low R:FR [48], indicating that increased auxin levels in EOD-FR-treated plants may be an important reason for upregulated XTH expression. Moreover, it has been shown that XTH9 expression increases significantly under low R:FR in *Arabidopsis* [62].

At present, XTHs are thought to be the main cell wall modifiers during plant response to low R:FR, but studies on *Arabidopsis* show that EXPs can enhance or supplement the function of XTHs [62]. Recent research shows that the expression of several EXP-related genes is upregulated after far-red light treatment in *Brassica napus*, further confirming the interaction between FR and EXPs [63]. Here, we identified 13 XTH genes and 12 EXP genes (Fig. 3), including XTH22 and XTH9. All were significantly upregulated after EOD-FR treatment, perhaps in response to apoplast acidification [64] induced by SAUR.

## Conclusion

In summary, we conclude that auxin plays an essential role in hypocotyl elongation mediated by EOD-FR treatment and propose the hypothetical mechanism presented in Fig. 9. EOD-FR treatment can significantly increase the expression of genes related to auxin synthesis, transport, and signal transduction. Our RNA-seq and metabolite profiles combined with previous studies suggest that the TAA-YUC pathway is both a low-R:FR-mediated auxin synthesis pathway and also the primary pathway by which EOD-FR promotes auxin synthesis. Our findings provide a new perspective on the role of auxin in hypocotyl elongation induced by EOD-FR and provide abundant resources for further investigation of the molecular mechanisms by which auxin controls plant growth in response to FR light.

## Methods

### Plant materials and sample collection

The *Cucurbita moschata* variety 'Shang 2' (Certification number: No. 2010001 of Shaanxi Vegetable Registration, provided by Shaanxi Academy of Agricultural Sciences, YangLing, China) was used as the experimental material. Seeds were soaked in hot water at 55 °C for 10 min with continuous stirring. When the water temperature dropped below 30 °C, the seeds were soaked for 6 hours. After the seeds had germinated in a constant temperature incubator at 30 °C, seedlings with the same sprouting length were sown into a 50-hole seedling plate and grown with seedling substrate. The plants were grown under artificial light (14 hours light at 28 °C, 10 hours dark at 18°C). After their hypocotyl hooks had emerged from the soil, the hypocotyls had straightened, and the cotyledons were fully unfolded, seedlings with

uniform growth were selected for use in the experiment. Twenty seedlings were used for each treatment, and the treatment durations and intensities are shown in Table 1. Four different treatments were set, far red light treatment(T), far red light plus inhibitor treatment(NPA-T), without far-red light treatment (CK) and inhibitor treatment(NPA-CK). The auxin inhibitor NPA (2  $\mu$ M) was applied 30 min before treatment. Hypocotyl lengths of all plants were measured daily with a steel ruler. The leaves and hypocotyls of eight plants were rapidly cut and frozen in liquid nitrogen for subsequent RNA sequencing and metabolite detection. After 6 days of treatment, six plants were randomly selected for measurement of plant height, stem diameter, and the dry and fresh weights of above- and belowground parts; three plants were used for the preparation of hypocotyl paraffin sections.

**Table 1.** Far-red light intensity (photon flux), duration, and applied far-red dose of the end-of-day far-red (EOD-FR) light

Treatment	Duration(s)	FR photo flux ( $\mu\text{mmol}\cdot\text{m}^{-2}\cdot\text{s}^{-1}$ )	FR dose ( $\text{mmol}\cdot\text{m}^{-2}\cdot\text{d}^{-1}$ )
CK	0	0	0
T	120	34	4.08
NPA-T	120	34	4.08
NPA-CK	0	0	0

### Auxin quantification

Auxin quantification was performed as described by Du et al [65] with minor modifications. Plant tissues stored at -80 °C were frozen in liquid nitrogen and crushed into a powder, then extracted with 1 mL methanol/water/formic acid (15:4:1, v/v/v). The combined extracts were evaporated to dryness under a nitrogen gas stream, reconstituted in 100  $\mu$ L 80% methanol (v/v), and filtered through a 0.22  $\mu$ m filter for further analysis.

The sample extracts were analyzed using an LC-ESI-MS/MS system (UHPLC, ExionLC™ AD; MS, Applied Biosystems 6500 Triple Quadrupole). The analytical conditions were as follows: HPLC column, Waters ACQUITY UPLC HSS T3 C18 (100 mm  $\times$  2.1 mm, 1.8  $\mu$ m); solvent system, water with 0.04% acetic acid (A) and acetonitrile with 0.04% acetic acid (B); gradient program, 5% B for 0–1 min, increased to 95% B over 1–8 min, 95% B for 8–9 min, reduced to 5% B over 9.1–12 min; 5  $\mu$ L sample supernatant or auxin standard injected into the HPLC with a 0.35 mL min<sup>-1</sup> flow rate at 40 °C. The effluent was alternately connected to an API 6500 QTRAP LC/MS/MS System equipped with an ESI Turbo Ion-Spray interface. The ESI source ran at 550 °C and a 5500 V ion spray voltage. The curtain gas was set at 35.0 pounds per square inch (psi), and the collision gas was set to medium. Declustering potential and collision energy for individual multiple reaction monitoring (MRM) transitions was performed with further optimization. A specific set of MRM transitions were monitored for each period based on the plant hormones eluted within this period. Three technical replicates and three biological replicates were injected into the HPLC

for auxin quantification. To verify the accurate identification and quantification of IAA, artificial checks of HPLC and ion results were conducted to identify the consistency of each sample. A standard curve with a regression coefficient >0.99 was used to calculate IAA levels.

## Metabolomics Profiling Analysis

Freeze-dried sample powder (0.1 g) of hypocotyl from CK and T were extracted with 50% methanol , then centrifuged and filtered at 4000 *g* and 4 °C. All chromatographic separations were performed using an ultra-performance liquid chromatography (UPLC) system (SCIEX, UK). An ACQUITY UPLC T3 column (100 mm × 2.1 mm, 1.8 µm, Waters, UK) was used for the reversed phase separation. A high-resolution tandem mass spectrometer TripleTOF 5600+ (SCIEX, UK) was used to detect metabolites eluted from the column. The Q-TOF was operated in both positive and negative ion modes. The mode of data collection was IDA (information dependent acquisition). To evaluate the stability of the LC-MS during the whole acquisition, a quality control sample (pooled from all samples) was run after every 10 experimental samples. The acquired MS data were pre-processed with XCMS software. LC-MS raw data files were converted into mzXML format and then processed using XCMS, CAMERA, and metaX toolbox implemented in R software. Each ion was identified by combining retention time (RT) and m/z removed. The MS fragment data from the mass spectrometer were matched with a secondary library of in-house metabolite standards, and metabolites with similarity >80% were extracted. An online database was used to annotate the metabolites by matching the exact molecular mass data (m/z) of the samples with those from the database. Statistical analysis was performed by *t*-test with multiple testing correction to obtain *Q*-values for individual metabolites, and VIP values were obtained using partial least squares discriminant analysis (PLS-DA). Significantly different metabolites were identified using thresholds of >2-fold difference, *Q*<0.05, and VIP >1.

## Transcriptome sequencing

CK and T were selected for RNA-SEQ analysis. Total RNA was extracted using Trizol reagent (Invitrogen, CA, USA) following the manufacturer's procedure. Then the RNA were reverse-transcribed to create 6 cDNA libraries in accordance with the protocol for the TruSeq Stranded mRNA Library Prep Kit (Illumina, San Diego, USA). And then we performed the paired-end sequencing on an Illumina Hiseq 4000 (LC-Bio Technology CO., Ltd., Hangzhou, China). Differential expression analysis was performed following previously described methods [66]. In brief, the fragments per kilobase per million reads (FPKM) method was used to calculate the expression levels of genes. The differentially expressed genes were selected with  $\log_2(\text{fold change}) > 1$  or  $\log_2(\text{fold change}) < -1$  and p value < 0.05 by the R package edgeR.

## Annotation and identification of DEGs

We annotated the DEGs by BLASTing against three public databases [NR(Non-Redundant Protein Sequence Database ), GO(Gene Ontology), and KEGG( Kyoto Encyclopedia of Genes and Genomes)]. DEGs were then subjected to GO functional enrichment analysis and KEGG pathway analysis by R. GO

terms or KEGG pathways with a Bonferroni-corrected P-value <0.05 were considered to be significantly enriched.

### **Integrated analysis of DEGs and differentially abundant metabolites**

To further clarify the relationships among DEGs, differentially abundant metabolites, and hypocotyl elongation, we calculated the Pearson correlations between key metabolites and key genes and created a corresponding heatmap.

### **Quantitative real-time PCR (qRT-PCR)**

Gene-specific primers for 14 genes were designed based on the sequences obtained from RNA-seq data (Additional file 6). At the end of the reaction, the dissociation curve was analyzed, and the specificity of the primers was evaluated. Actin primers used were the

following: CmaActin\_Forward:CTGCTGAGATGAACAAAAGGTC, CmaActin\_Reverse: TGTGCAGTAGTACTTGGTGGTCTC. Relative gene expression levels were

calculated using the  $2^{-\Delta\Delta Ct}$  method [67]. All reactions in all experiments were repeated three times.

### **Preparation and observation of hypocotyl paraffin sections**

Three hypocotyls were fixed in FAA (3.7% formaldehyde, 5% acetic acid, and 50% ethanol, by vol.) fixative for more than 24 hours under vacuum. The fixed tissues were then dehydrated in an ethanol series (70, 80, and 90%) and processed as described [68]. Wax blocks were sectioned at 10  $\mu$ m. Safranin-O/fast-green staining was performed using a kit following manufacturer's instructions (Wuhan Google Bio-Technology Co., Wuhan, China). Used the research-grade upright fluorescence microscope (BX51, Olympus Corporation, Japan) to observe and photograph the cell. The software used to observe and measure cells was CellSens Standard, magnification of 20X.

### **Statistical Analysis of Data**

All data were analyzed by GraphPad Prism 8, Excel 2013, and SPSS19.0, the expressed as mean $\pm$ SD. Statistical analyses were conducted using Student's t test. P values less than 0.05 were considered statistically significant.

## **Abbreviations**

EOD-FR: end-of-day far-red; IAA: indole-3-acetic acid; PAT: polar auxin transport;

RNA-Seq: transcriptome sequencing; FPKM: fragments per kilobase per million

reads; LC-MS/MS: metabolomics; VIP: variable importance in projection; PCA:

principal component analysis; qRT-PCR: quantitative real-time PCR; DEGs: differentially expressed genes; GO: Gene Ontology; KEGG: Kyoto Encyclopedia of Genes and Genomes; NR: NCBI Refseq; XTH: endotransglucosylase/hydrolases; EXP: expansin; TAA1: L-tryptophan—pyruvate aminotransferase; TAR2: tryptophan aminotransferase related 2; YUCCA: indole-3-pyruvate monooxygenase; trpF: phosphoribosylanthranilate isomerase; PIN: pin-formed protein; PILS: pin-likes protein; ABCB: ATP-binding cassette: subfamily B; AUX/LAX: auxin influx carrier; WAT1: Protein WALLS ARE THIN 1; CIPK: CBL-interacting protein kinase; AUX/IAA: auxin-responsive protein IAA; GH3: Gretchen Hagen 3; SAUR: Small Auxin Up RNA; ILR1: IAA-amino acid hydrolase; ABP1: auxin binding protein 1.

## Declarations

### Ethics approval and consent to participate

Not applicable.

### Consent for publication

Not applicable.

### Availability of data and materials

The transcriptome data and metabolomics data associated with this article were uploaded for supplementary data. Other datasets are available from the corresponding author on a reasonable request.

### Competing interests

The authors declare that they have no competing interests.

### Funding

This work was supported by the National Key Research and Development Project (2018YFD0201205-2), Shaanxi Province Agricultural Science and Technology Innovation Integration Promotion Project (NYKJ-2018-YL22) and Shaanxi Province Technical Innovation Guidance Special Project (2021-YD-QFY-0094).

Purchase of experimental materials, cost of auxin, transcriptome data and metabolomics data determination were funded by 2018YFD0201205-2 and NYKJ-2018-YL22. The purchase of experimental

instruments and writing the manuscript were funded by 2021-YD-QFY-0094.

## Authors' contributions

ZY and YW designed the experiments. QL and HZ performed the experiments. YM, QL, JM, XX and HY collected the samples. QL and YB drafted the manuscript. ZY and YW proofread and finalized the manuscript. All authors have read and approved the final manuscript.

## Acknowledgements

Not applicable.

## Author details

<sup>1</sup>College of Horticulture Northwest A&F University Yangling 712100, Shaanxi, China

<sup>2</sup>College of Sciences, Northwest A&F University, Yangling 712100, Shaanxi, China

<sup>3</sup>Northwest A&F University/Key Laboratory of Protected Horticultural Engineering in Northwestern China, Ministry of Agriculture and Rural Affairs, Yangling 712100, Shaanxi, China

## References

1. Chia PL, Kubota C. End-of-day Far-red Light Quality and Dose Requirements for Tomato Rootstock Hypocotyl Elongation. *Hortscience*. 2010;45(10):1501-1506.
2. Louws FJ, Rivard CL, Kubota C. Grafting fruiting vegetables to manage soilborne pathogens, foliar pathogens, arthropods and weeds. *Scientia Horticulturae*. 2010;127(2):127-146.
3. Yang ZC, Kubota C, Chia PL, Kacira M. Effect of end-of-day far-red light from a movable LED fixture on squash rootstock hypocotyl elongation. *Scientia Horticulturae*. 2012;136:81-86.
4. Jiao Y, Lau OS, Deng XW. Light-regulated transcriptional networks in higher plants. *Nature Reviews Genetics*. 2007;8(3):217-230.
5. Kong Y, Schiestel K, Zheng Y. Maximum elongation growth promoted as a shade-avoidance response by blue light is related to deactivated phytochrome: a comparison with red light in four microgreen species. *Canadian Journal of Plant Science*. 2020;100(3):314-326.
6. Song J, Cao K, Hao Y, Song S, Su W, Liu H. Hypocotyl elongation is regulated by supplemental blue and red light in cucumber seedling. *Gene*. 2019;707:117-125.
7. Bantis F, Smirnakou S, Ouzounis T, Koukounaras A, Ntagkas N, Radoglou K. Current status and recent achievements in the field of horticulture with the use of light-emitting diodes (LEDs). *Scientia Horticulturae*. 2018;235:437-451.
8. Xiong JQ, Patil GG, Moe R. Effect of DIF and end-of-day light quality on stem elongation in *Cucumis sativus*. *Scientia Horticulturae*. 2002;94(3-4):219-229.

9. Graham HAH, Decoteau DR. Young watermelon plant growth responses to end-of-day red and far-red light are affected by direction of exposure and plant part exposed. *Scientia Horticulturae*. 1997;69(1-2):41-49.
10. Bognar LK, Hall A, Adam E, Thain SC, Nagy F, Millar AJ. The circadian clock controls the expression pattern of the circadian input photoreceptor, phytochrome B. *Proceedings of the National Academy of Sciences of the United States of America*. 1999;96(25):14652-14657.
11. Rockwell NC, Su Y-S, Lagarias JC. Phytochrome structure and signaling mechanisms. *Annual Review of Plant Biology*. 2006;57:837-858.
12. Khanna R, Huq E, Kikis EA, Al-Sady B, Lanzatella C, Quail PH. A novel molecular recognition motif necessary for targeting photoactivated phytochrome signaling to specific basic helix-loop-helix transcription factors. *Plant Cell*. 2004;16(11):3033-3044.
13. Carriero LG, Maloof JN, Brady SM. Molecular control of crop shade avoidance. *Current Opinion in Plant Biology*. 2016;30:151-158.
14. Franklin KA. Shade avoidance. *New Phytologist*. 2008;179(4):930-944.
15. Yang C, Li L. Hormonal Regulation in Shade Avoidance. *Frontiers in Plant Science*. 2017;8.
16. Tao Y, Ferrer JL, Ljung K, Pojer F, Hong F, Long JA, Li L, Moreno JE, Bowman ME, Ivans LJ *et al*. Rapid synthesis of auxin via a new tryptophan-dependent pathway is required for shade avoidance in plants. *Cell*. 2008;133(1):164-176.
17. Zheng Z, Guo Y, Novak O, Chen W, Ljung K, Noel JP, Chory J. Local auxin metabolism regulates environment-induced hypocotyl elongation. *Nature Plants*. 2016;2(4).
18. Takemura Y, Kuroki K, Katou M, Kishimoto M, Tsuji W, Nishihara E, Tamura F. Gene expression changes triggered by end-of-day far-red light treatment on early developmental stages of *Eustoma grandiflorum* (*Raf.*) Shinn. *Scientific Reports*. 2015;5.
19. Schwender J, Koenig C, Klapperstueck M, Heinzel N, Munz E, Hebbelmann I, Hay JO, Denolf P, De Bodt S, Redestig H *et al*. Transcript abundance on its own cannot be used to infer fluxes in central metabolism. *Frontiers in Plant Science*. 2014;5.
20. Bino RJ, Hall RD, Fiehn O, Kopka J, Saito K, Draper J, Nikolau BJ, Mendes P, Roessner-Tunali U, Beale MH *et al*. Potential of metabolomics as a functional genomics tool. *Trends in Plant Science*. 2004;9(9):418-425.
21. Karaagac O, Balkaya A: Interspecific hybridization and hybrid seed yield of winter squash (*Cucurbita maxima* Duch.) and pumpkin (*Cucurbita moschata* Duch.) lines for rootstock breeding. *Scientia Horticulturae*. 2013;149:9-12.
22. Maeda H, Dudareva N: The Shikimate Pathway and Aromatic Amino Acid Biosynthesis in Plants. In: Annual Review of Plant Biology, Vol 63. Edited by Merchant SS, vol. 63. 2012;73-105.
23. Sasidharan R, Voesenek LACJ, Pierik R. Cell Wall Modifying Proteins Mediate Plant Acclimatization to Biotic and Abiotic Stresses. *Critical Reviews in Plant Sciences*. 2011;30(6):548-562.

24. Cosgrove DJ. New genes and new biological roles for expansins. *Current Opinion in Plant Biology.* 2000;3(1):73-78.
25. Fry SC. POLYSACCHARIDE-MODIFYING ENZYMES IN THE PLANT-CELL WALL. *Annual Review of Plant Physiology and Plant Molecular Biology.* 1995;46:497-520.
26. Won C, Shen X, Mashiguchi K, Zheng Z, Dai X, Cheng Y, Kasahara H, Kamiya Y, Chory J, Zhao Y. Conversion of tryptophan to indole-3-acetic acid by TRYPTOPHAN AMINOTRANSFERASES OF ARABIDOPSIS and YUCCAs in Arabidopsis. *Proceedings of the National Academy of Sciences of the United States of America.* 2011;108(45):18518-18523.
27. Yamamoto Y, Kamiya N, Morinaka Y, Matsuoka M, Sazuka T. Auxin biosynthesis by the YUCCA genes in rice. *Plant Physiology.* 2007;143(3):1362-1371.
28. Zhao YD, Christensen SK, Fankhauser C, Cashman JR, Cohen JD, Weigel D, Chory J. A role for flavin monooxygenase-like enzymes in auxin biosynthesis. *Science.* 2001;291(5502):306-309.
29. Mashiguchi K, Tanaka K, Sakai T, Sugawara S, Kawaide H, Natsume M, Hanada A, Yaeno T, Shirasu K, Yao H *et al.* The main auxin biosynthesis pathway in Arabidopsis. *Proceedings of the National Academy of Sciences of the United States of America.* 2011;108(45):18512-18517.
30. Muller-Moule P, Nozue K, Pytlak ML, Palmer CM, Covington MF, Wallace AD, Harmer SL, Maloof JN. YUCCA auxin biosynthetic genes are required for Arabidopsis shade avoidance. *PeerJ.* 2016;
31. Matsuda F, Yamada T, Miyazawa H, Miyagawa H, Wakasa K. Characterization of tryptophan-overproducing potato transgenic for a mutant rice anthranilate synthase alpha-subunit gene (OASA1D). *Planta.* 2005;222(3):535-545.
32. Morino K, Matsuda F, Miyazawa H, Sukegawa A, Miyagawa H, Wakasa K. Metabolic profiling of tryptophan-overproducing rice calli that express a feedback-insensitive alpha subunit of anthranilate synthase. *Plant and Cell Physiology.* 2005;46(3):514-521.
33. Grones P, Friml J. Auxin transporters and binding proteins at a glance. *Journal of Cell Science.* 2015;128(1):1-7.
34. Keuskamp DH, Pollmann S, Voesenek LACJ, Peeters AJM, Pierik R. Auxin transport through PIN-FORMED 3 (PIN3) controls shade avoidance and fitness during competition. *Proceedings of the National Academy of Sciences of the United States of America* 2010;107(52):22740-22744.
35. Barbez E, Kubes M, Rolcik J, Beziat C, Pencik A, Wang B, Rosquete MR, Zhu J, Dobrev PI, Lee Y *et al.* A novel putative auxin carrier family regulates intracellular auxin homeostasis in plants. *Nature.* 2012;485(7396):119-U155.
36. Beziat C, Barbez E, Feraru MI, Lucyshyn D, Kleine-Vehn J. Light triggers PILS-dependent reduction in nuclear auxin signalling for growth transition. *Nature Plants.* 2017;3(8).
37. Geisler M, Murphy AS. The ABC of auxin transport: The role of p-glycoproteins in plant development. *Febs Letters.* 2006;580(4):1094-1102.
38. Ge Y, Yan F, Zourelidou M, Wang M, Ljung K, Fastner A, Hammes UZ, Di Donato M, Geisler M, Schwechheimer C *et al.* SHADE AVOIDANCE 4 Is Required for Proper Auxin Distribution in the Hypocotyl. *Plant Physiology.* 2017;173(1):788-800.

39. Wu G, Carville JS, Spalding EP. ABCB19-mediated polar auxin transport modulates Arabidopsis hypocotyl elongation and the endoreplication variant of the cell cycle. *Plant Journal*. 2016;85(2):209-218.
40. Titapiwatanakun B, Blakeslee JJ, Bandyopadhyay A, Yang H, Mravec J, Sauer M, Cheng Y, Adamec J, Nagashima A, Geisler M *et al*. ABCB19/PGP19 stabilises PIN1 in membrane microdomains in Arabidopsis. *Plant Journal*. 2009;57(1):27-44.
41. Hoyerova K, Perry L, Hand P, Lankova M, Kocabek T, May S, Kottova J, Paces J, Napier R, Zazimalova E. Functional characterization of PaLAX1, a putative auxin permease, in heterologous plant systems. *Plant Physiology*. 2008;146(3):1128-1141.
42. Aryal B, Jonsson K, Baral A, Sancho-Andres G, Routier-Kierzkowska A-L, Kierzkowski D, Bhalerao RP. Interplay between Cell Wall and Auxin Mediates the Control of Differential Cell Elongation during Apical Hook Development. *Current Biology*. 2020;30(9):1733-+.
43. Ranocha P, Dima O, Nagy R, Felten J, Corratge-Faillie C, Novak O, Morreel K, Lacombe B, Martinez Y, Pfrunder S *et al*. Arabidopsis WAT1 is a vacuolar auxin transport facilitator required for auxin homoeostasis. *Nature Communications*. 2013;
44. Tripathi V, Parasuraman B, Laxmi A, Chattopadhyay D. CIPK6, a CBL-interacting protein kinase is required for development and salt tolerance in plants. *Plant Journal*. 2009;58(5):778-790.
45. Leyser O. Auxin Signaling. *Plant Physiology*. 2018;176(1):465-479.
46. Salehin M, Bagchi R, Estelle M. SCFTIR1/AFB-Based Auxin Perception: Mechanism and Role in Plant Growth and Development. *Plant Cell* 2015;27(1):9-19.
47. Abel S, Theologis A. Early genes and auxin action. *Plant Physiology*. 1996;111(1):9-17.
48. Kozuka T, Kobayashi J, Horiguchi G, Demura T, Sakakibara H, Tsukaya H, Nagatani A. Involvement of Auxin and Brassinosteroid in the Regulation of Petiole Elongation under the Shade. *Plant Physiology*. 2010;153(4):1608-1618.
49. Pucciariello O, Legris M, Costigliolo Rojas C, Jose Iglesias M, Esteban Hernando C, Dezar C, Vazquez M, Yanovsky MJ, Finlayson SA, Prat S *et al*. Rewiring of auxin signaling under persistent shade. *Proceedings of the National Academy of Sciences of the United States of America*. 2018;115(21):5612-5617.
50. Yang C, Xie F, Jiang Y, Li Z, Huang X, Li L. Phytochrome A Negatively Regulates the Shade Avoidance Response by Increasing Auxin/Indole Acidic Acid Protein Stability. *Developmental Cell*. 2018;44(1):29-+.
51. Vandebussche F, Vriezen WH, Smalle J, Laarhoven LJJ, Harren FJM, Van Der Straeten D: Ethylene and auxin control the Arabidopsis response to decreased light intensity. *Plant Physiology* 2003, 133(2):517-527.
52. Nakazawa M, Yabe N, Ichikawa T, Yamamoto YY, Yoshizumi T, Hasunuma K, Matsui M. DFL1, an auxin-responsive GH3 gene homologue, negatively regulates shoot cell elongation and lateral root formation, and positively regulates the light response of hypocotyl length. *Plant Journal*. 2001;25(2):213-221.

53. Spartz AK, Ren H, Park MY, Grandt KN, Lee SH, Murphy AS, Sussman MR, Overvoorde PJ, Gray WM. SAUR Inhibition of PP2C-D Phosphatases Activates Plasma Membrane H<sup>+</sup>-ATPases to Promote Cell Expansion in Arabidopsis. *Plant Cell*. 2014;26(5):2129-2142.
54. Du M, Spalding EP, Gray WM. Rapid Auxin-Mediated Cell Expansion. *Annual review of plant biology*. 2020;71:379-402.
55. Qiu T, Chen Y, Li M, Kong Y, Zhu Y, Han N, Bian H, Zhu M, Wang J. The tissue-specific and developmentally regulated expression patterns of the SAUR41 subfamily of SMALL AUXIN UP RNA genes: Potential implications. *Plant Signaling & Behavior*. 2013;8(8):e25283-Article No.: e25283.
56. Sun N, Wang J, Gao Z, Dong J, He H, Terzaghi W, Wei N, Deng XW, Chen H. Arabidopsis SAURs are critical for differential light regulation of the development of various organs. *Proceedings of the National Academy of Sciences of the United States of America*. 2016;113(21):6071-6076.
57. Gallei M, Luschnig C, Friml J. Auxin signalling in growth: Schrodinger's cat out of the bag. *Current Opinion in Plant Biology*. 2020;53:43-49.
58. Robert S, Kleine-Vehn J, Barbez E, Sauer M, Paciorek T, Baster P, Vanneste S, Zhang J, Simon S, Covanova M *et al.* ABP1 Mediates Auxin Inhibition of Clathrin-Dependent Endocytosis in Arabidopsis. *Cell*. 2010;143(1):111-121.
59. Effendi Y, Jones AM, Scherer GFE. AUXIN-BINDING-PROTEIN1 (ABP1) in phytochrome-B-controlled responses. *Journal of Experimental Botany*. 2013;64(16):5065-5074.
60. Rose JKC, Braam J, Fry SC, Nishitani K. The XTH family of enzymes involved in xyloglucan endotransglucosylation and endohydrolysis: Current perspectives and a new unifying nomenclature. *Plant and Cell Physiology*. 2002;43(12):1421-1435.
61. Cosgrove DJ. Loosening of plant cell walls by expansins. *Nature*. 2000;407(6802):321-326.
62. Sasidharan R, Chinnappa CC, Staal M, Elzenga JTM, Yokoyama R, Nishitani K, Voesenek LACJ, Pierik R. Light Quality-Mediated Petiole Elongation in Arabidopsis during Shade Avoidance Involves Cell Wall Modification by Xyloglucan Endotransglucosylase/Hydrolases. *Plant Physiology*. 2010;154(2):978-990.
63. Muthusamy M, Kim JA, Jeong MJ, Lee SI. Blue and red light upregulate alpha-expansin 1 (EXPA1) in transgenic *Brassica rapa* and its overexpression promotes leaf and root growth in Arabidopsis. *Plant Growth Regulation*. 2020;91(1):75-87.
64. Ivakov A, Flis A, Apelt F, Fuenfgeld M, Scherer U, Stitt M, Kragler F, Vissenberg K, Persson S, Suslov D. Cellulose Synthesis and Cell Expansion Are Regulated by Different Mechanisms in Growing Arabidopsis Hypocotyls. *Plant Cell*. 2017;29(6):1305-1315.
65. Du F, Ruan G, Liu H: Analytical methods for tracing plant hormones (vol 403, pg 55, 2012). *Analytical and Bioanalytical Chemistry*. 2012;404(5):1615-1615.
66. Trapnell C, Williams BA, Pertea G, Mortazavi A, Kwan G, van Baren MJ, Salzberg SL, Wold BJ, Pachter L. Transcript assembly and quantification by RNA-Seq reveals unannotated transcripts and isoform switching during cell differentiation. *Nature Biotechnology*. 2010;28(5):511-U174.

67. Schmittgen TD, Livak KJ. Analyzing real-time PCR data by the comparative C-T method. *Nature Protocols*. 2008;3(6):1101-1108.
68. Jing W, Zhang S, Fan Y, Deng Y, Wang C, Lu J, Sun X, Ma N, Shahid MO, Li Y *et al*. Molecular Evidences for the Interactions of Auxin, Gibberellin, and Cytokinin in Bent Peduncle Phenomenon in Rose (*Rosa sp.*). *International Journal of Molecular Sciences*. 2020;21(4).

## Figures

a

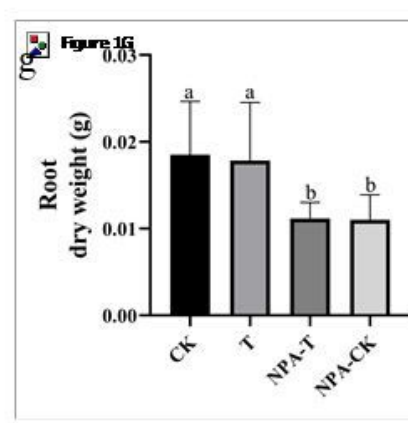
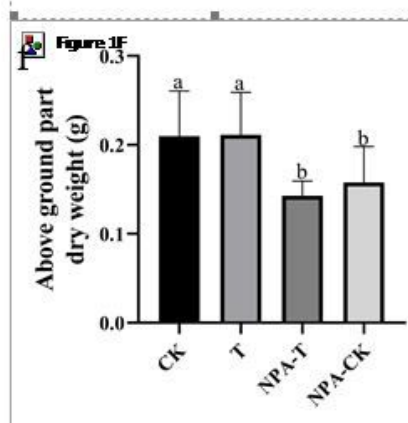
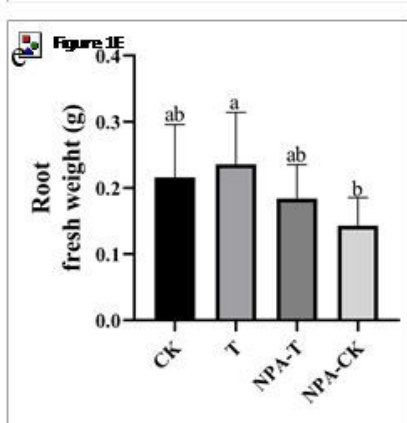
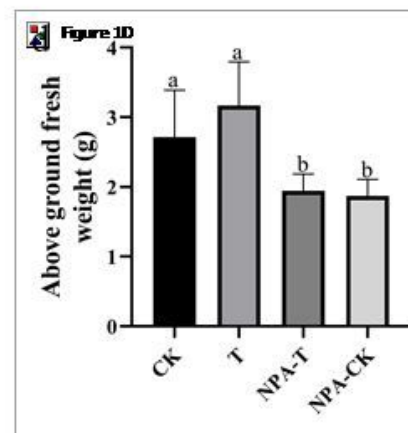
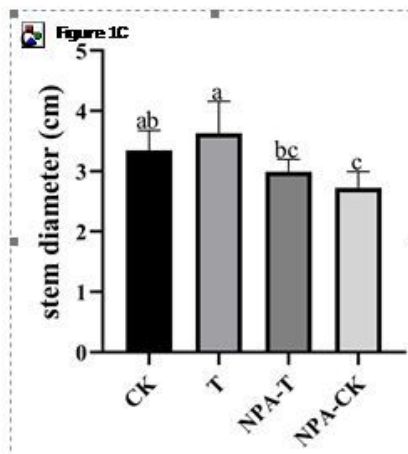
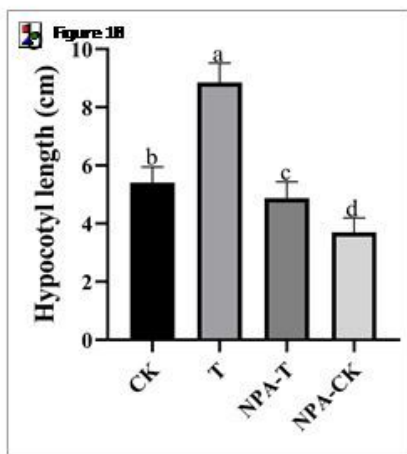


**Figure 1**

Change of plant Phenotype of pumpkin seedling during EOD-FR treatment.(a) Pumpkin seedlings during different treatments. Hypocotyl length (b),stem diameter(c),above ground fresh weight (d), root fresh weight (e),above ground dry weight (f), root dry weight (g) of pumpkin seedlings during different treatments. Error bars represent  $\pm$ SD. Different letters denote significant differences ( $p < 0.05$ ).

a

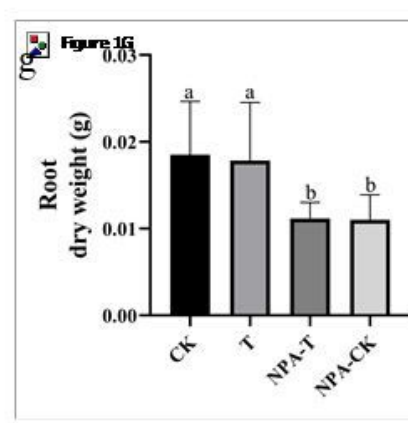
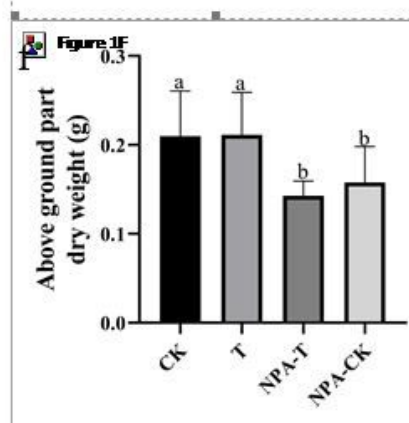
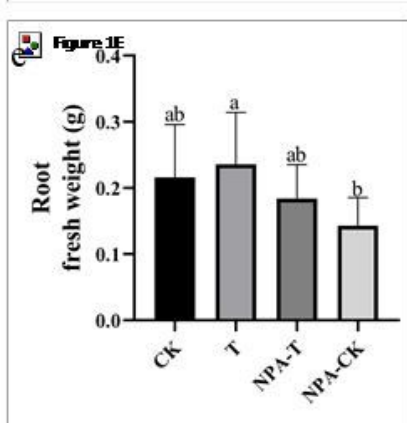
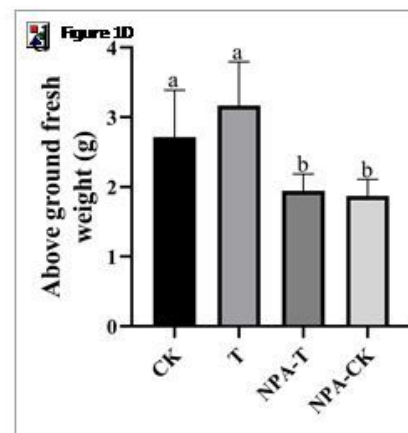
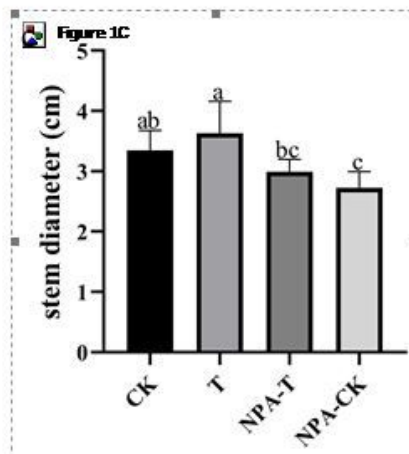
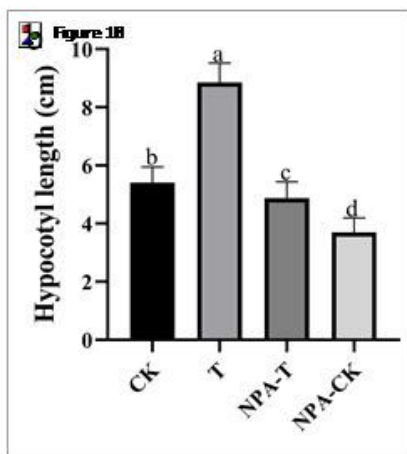


**Figure 1**

Change of plant Phenotype of pumpkin seedling during EOD-FR treatment.(a) Pumpkin seedlings during different treatments. Hypocotyl length (b),stem diameter(c),above ground fresh weight (d), root fresh weight (e),above ground dry weight (f), root dry weight (g) of pumpkin seedlings during different treatments. Error bars represent  $\pm$ SD. Different letters denote significant differences ( $p < 0.05$ ).

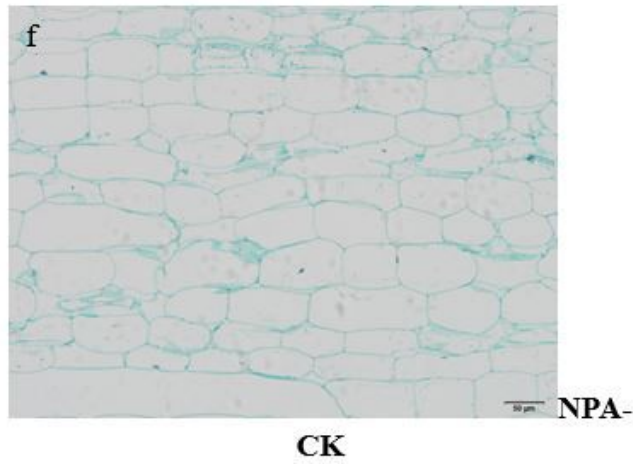
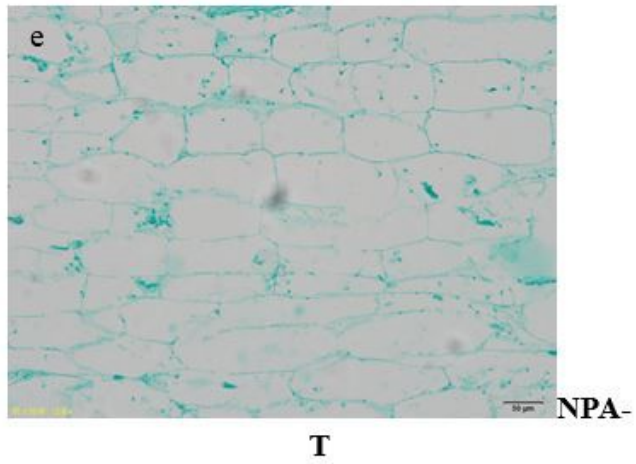
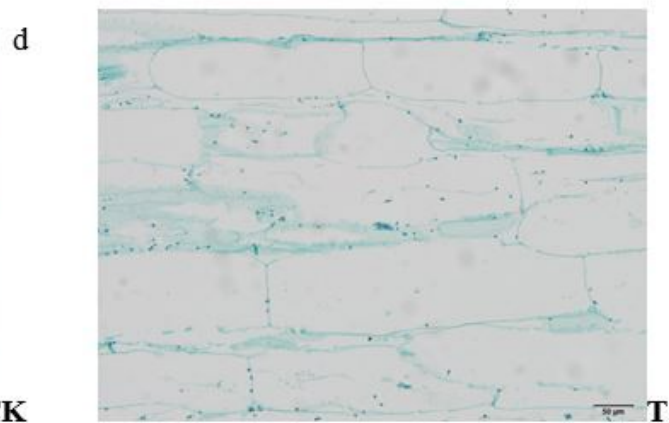
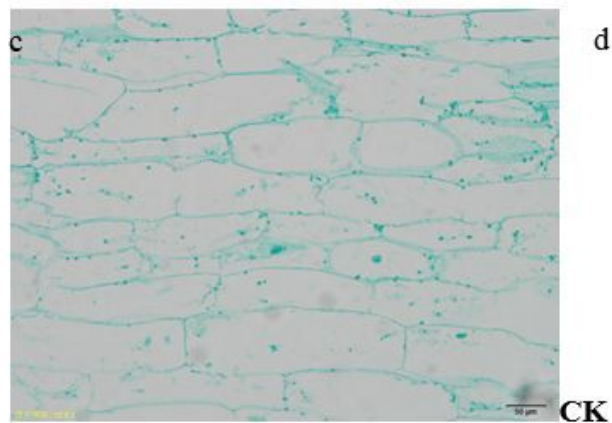
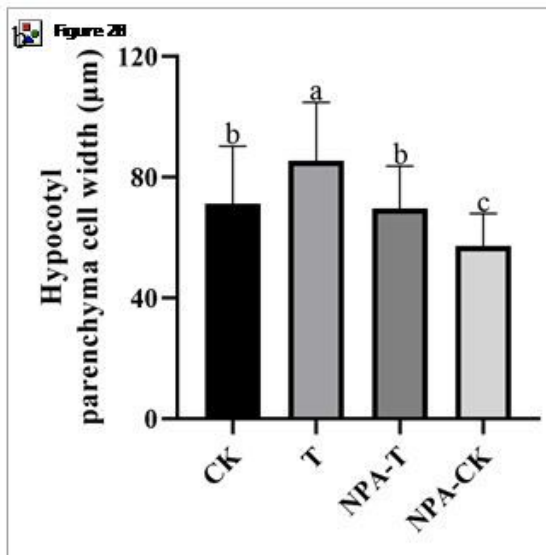
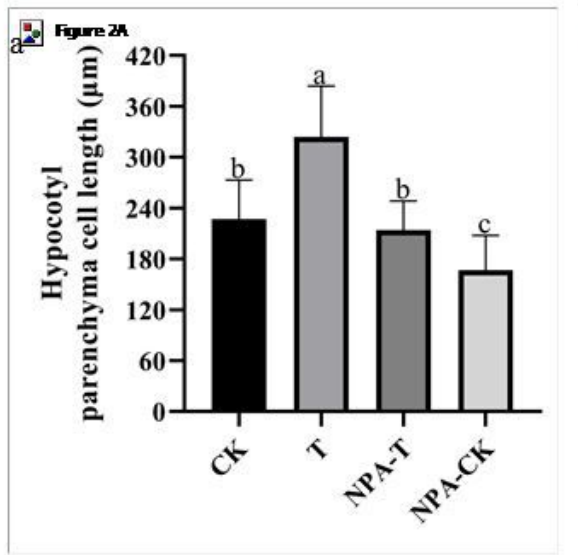


**Figure 2**

Observation on hypocotyl cells of pumpkin seedlings during EOD-FR treatment. Changes in length (a) and width (b) of parenchyma cells during different treatments. Error bars represent  $\pm\text{SD}$ . Different letters denote significant differences ( $p < 0.05$ ). Morphological changes of hypocotyl cells among different treatments (c, d, e and f)

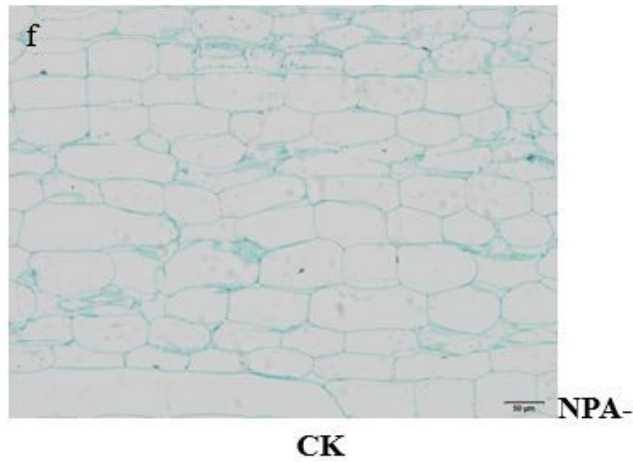
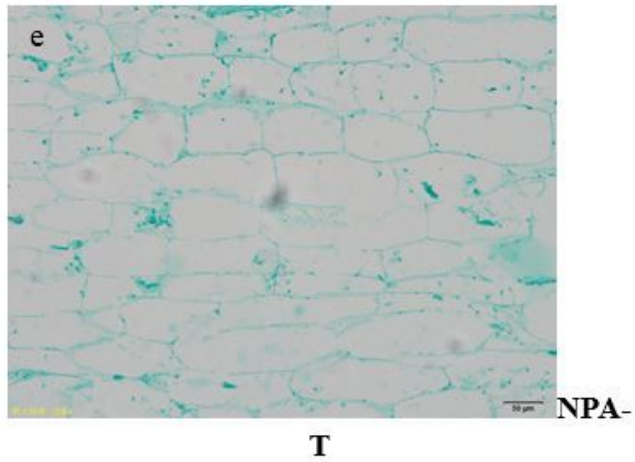
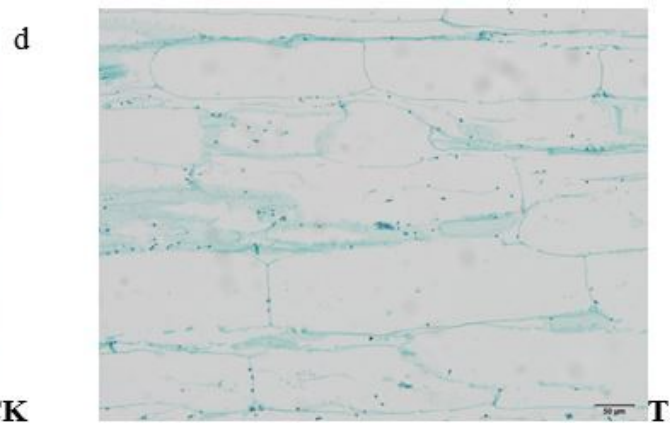
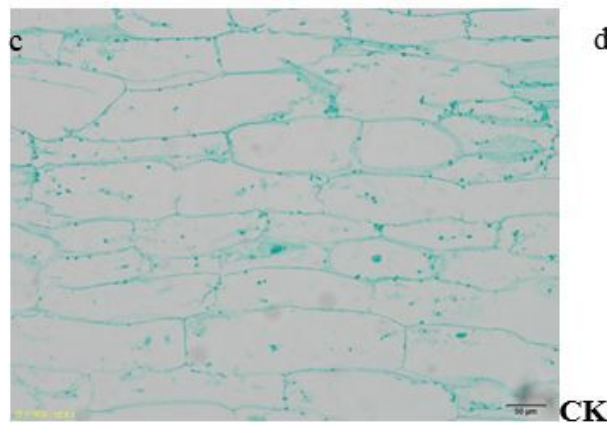
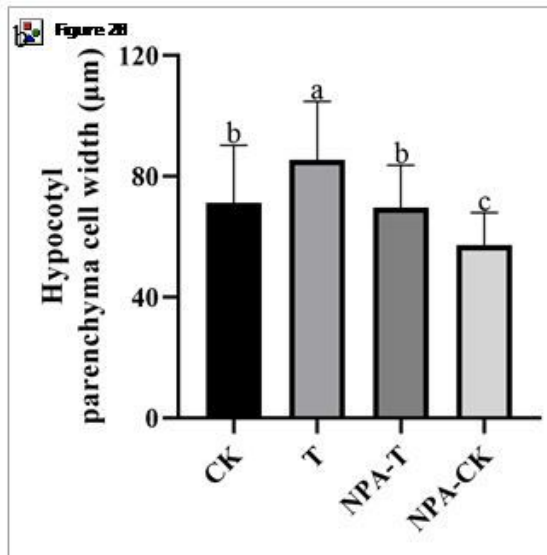
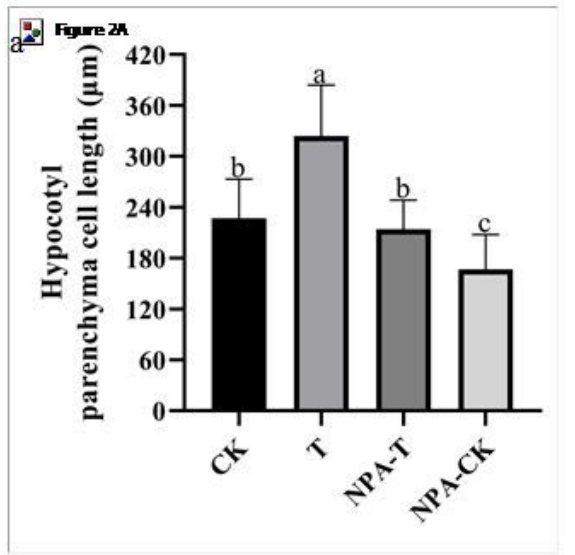


**Figure 2**

Observation on hypocotyl cells of pumpkin seedlings during EOD-FR treatment. Changes in length (a) and width (b) of parenchyma cells during different treatments. Error bars represent  $\pm\text{SD}$ . Different letters denote significant differences ( $p < 0.05$ ). Morphological changes of hypocotyl cells among different treatments (c, d, e and f)

# IAA Concentration

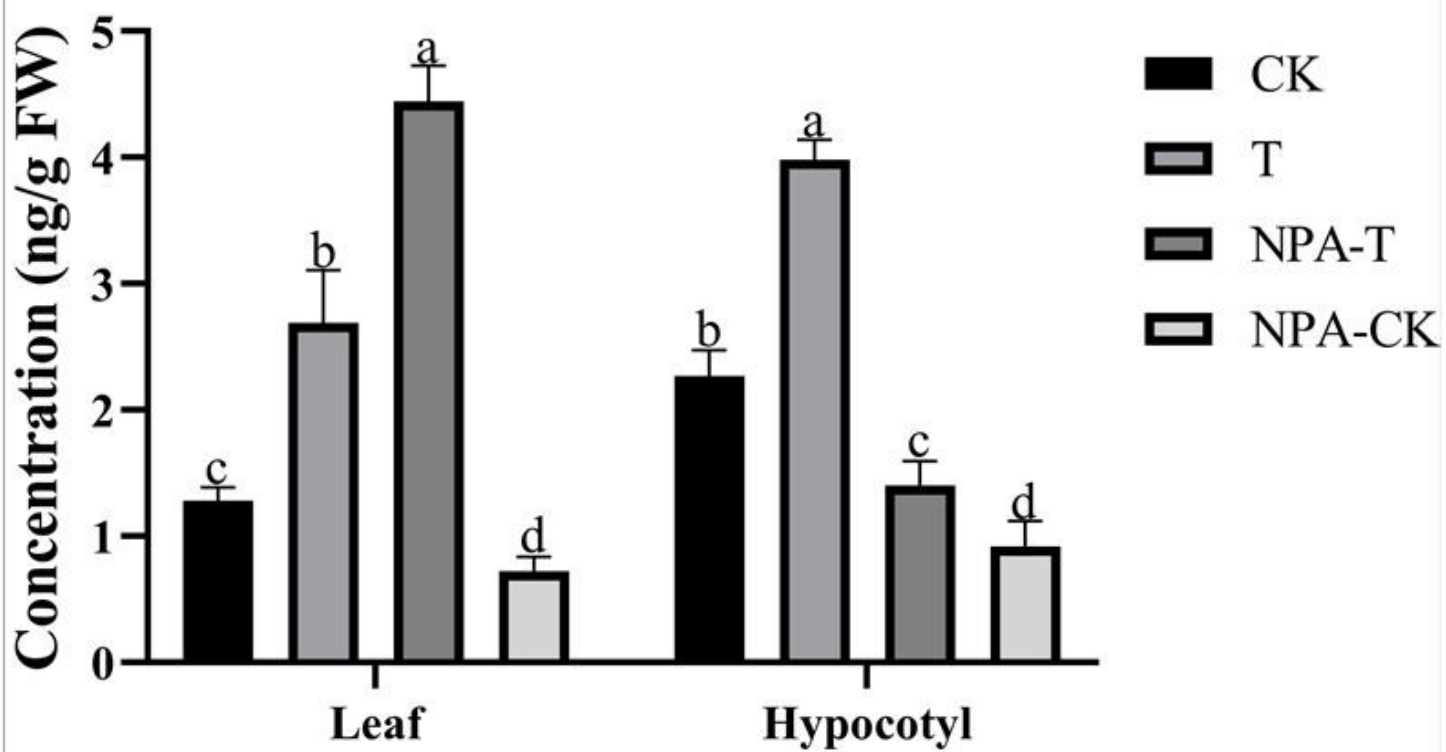


Figure 3

IAA levels in different treatments. Error bars represent  $\pm$ SD. Different letters denote significant differences ( $P < 0.05$ ).

# IAA Concentration

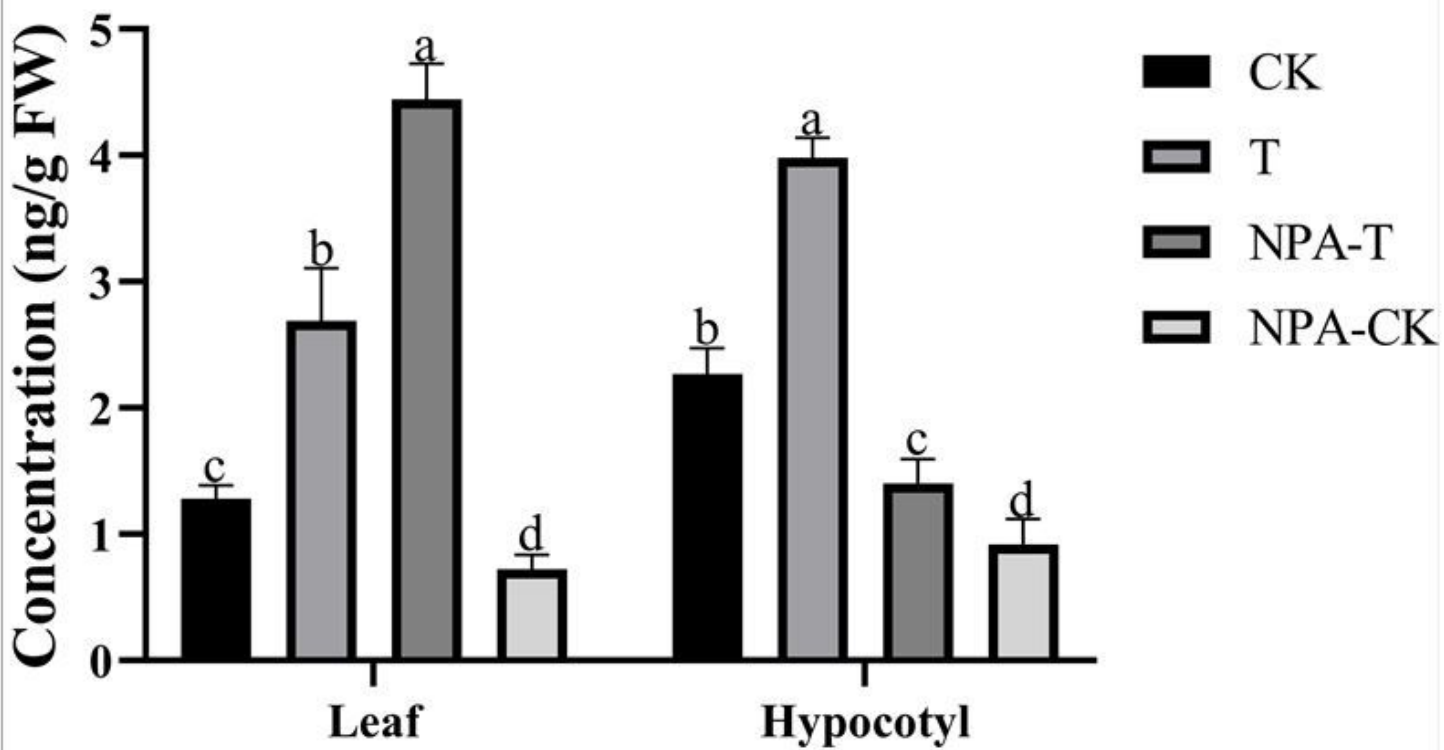
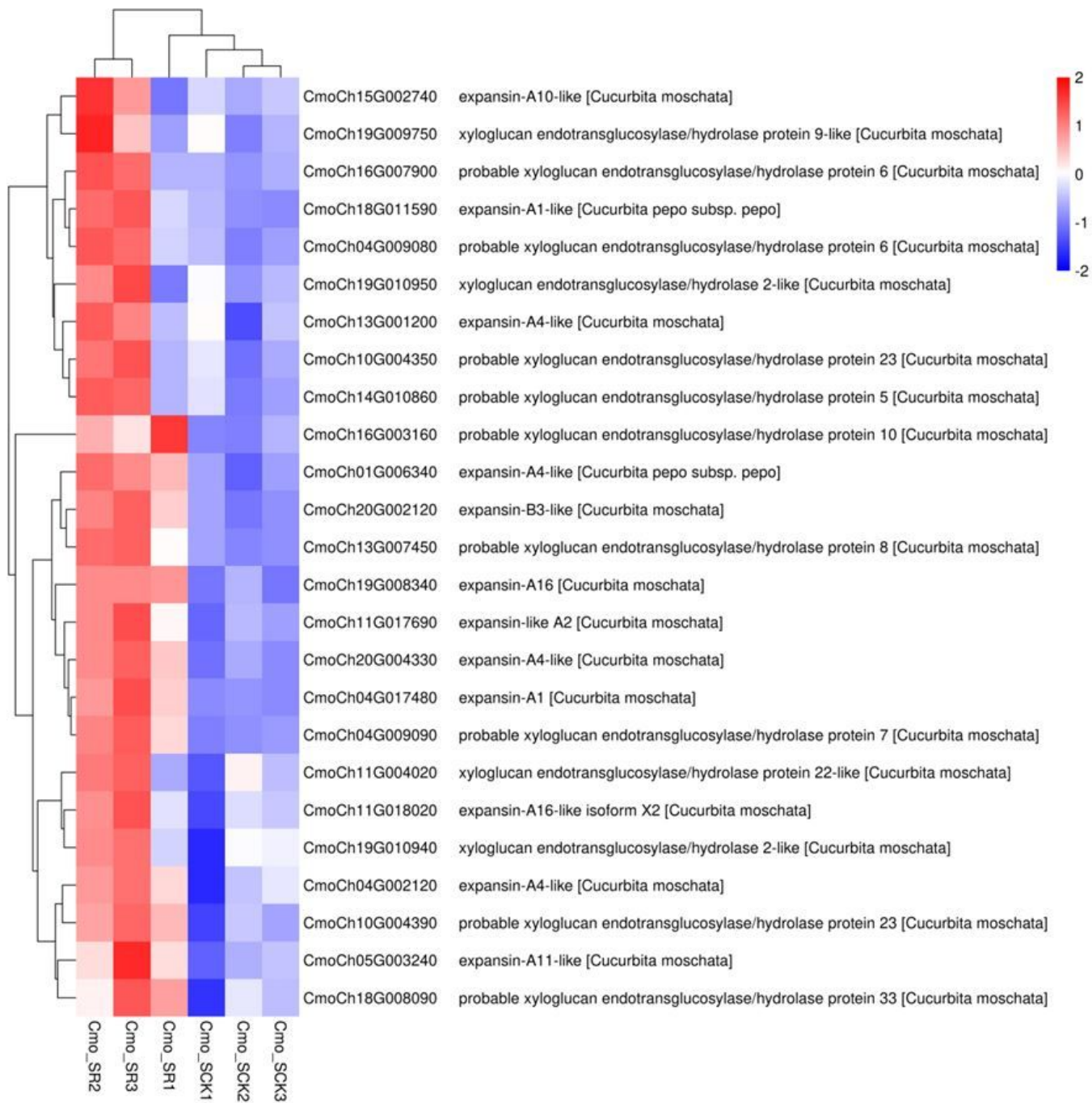


Figure 3

IAA levels in different treatments. Error bars represent  $\pm$ SD. Different letters denote significant differences ( $P < 0.05$ ).



**Figure 4**

Expression heatmap of DEGs related to cell wall proteins in pumpkin during EOD-FR treatment.

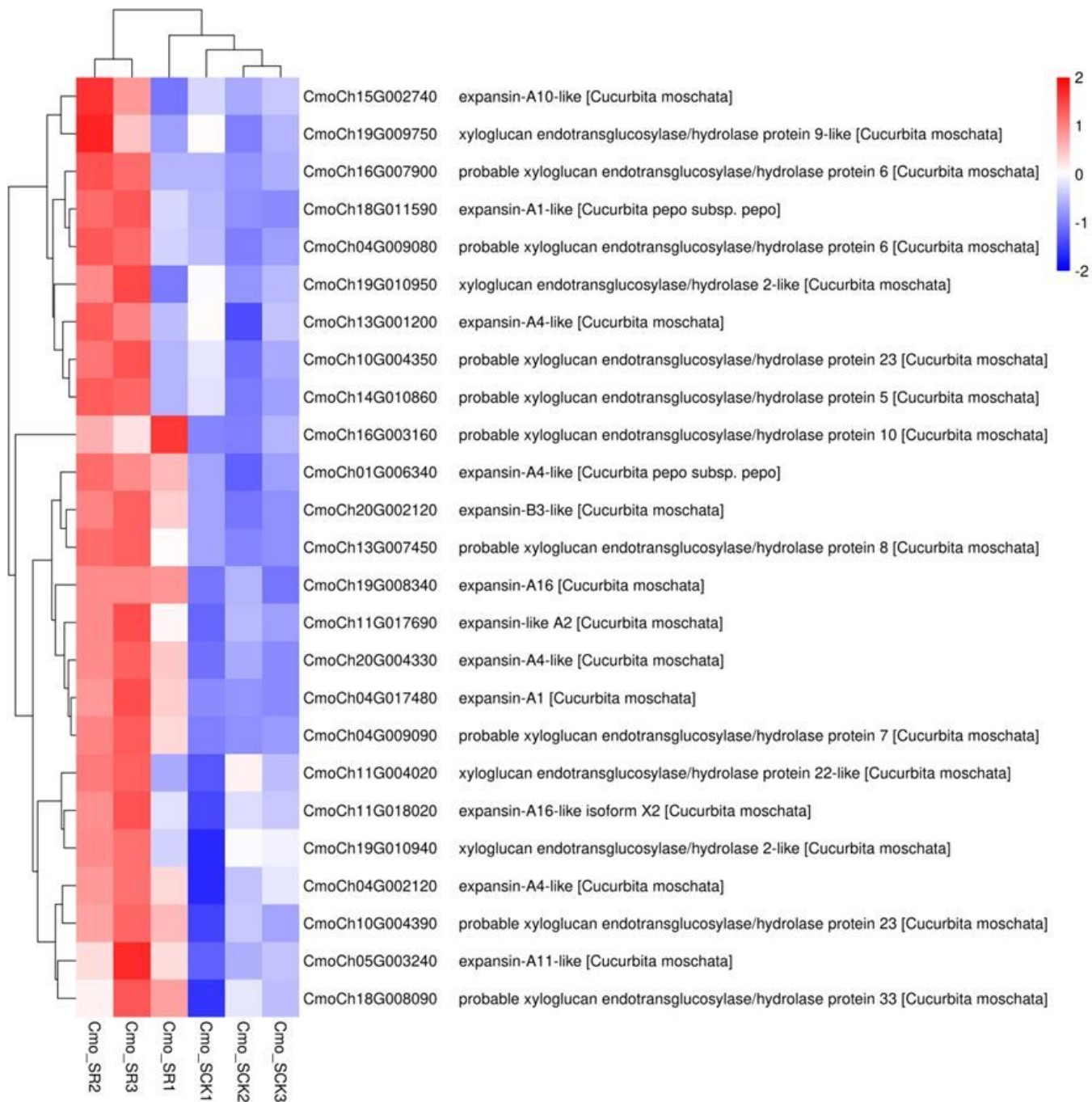


**Figure 4**

Expression heatmap of DEGs related to cell wall proteins in pumpkin during EOD-FR treatment.

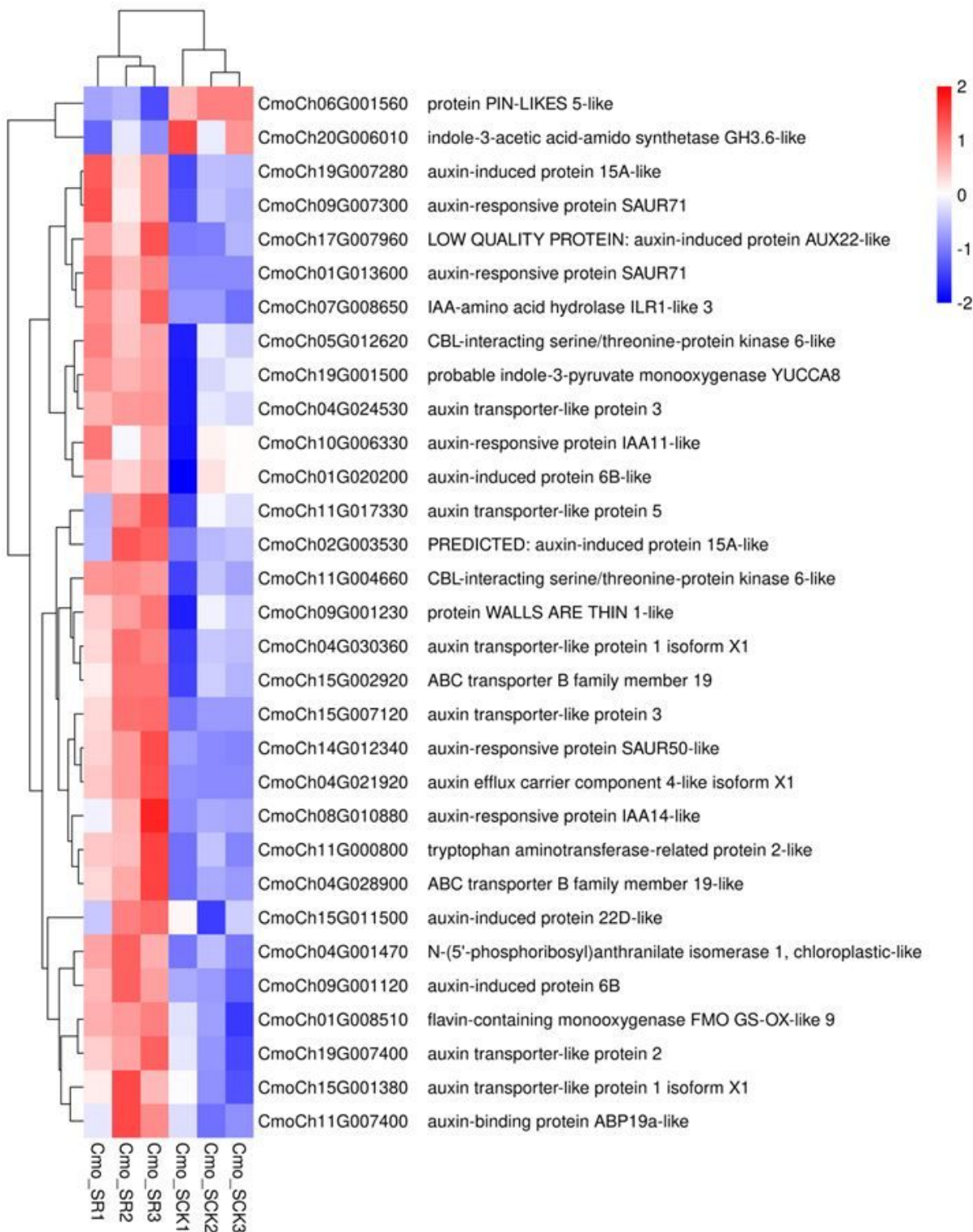


**Figure 5**

Expression heatmap of DEGs related to auxin response in pumpkin during EOD-FR treatment.

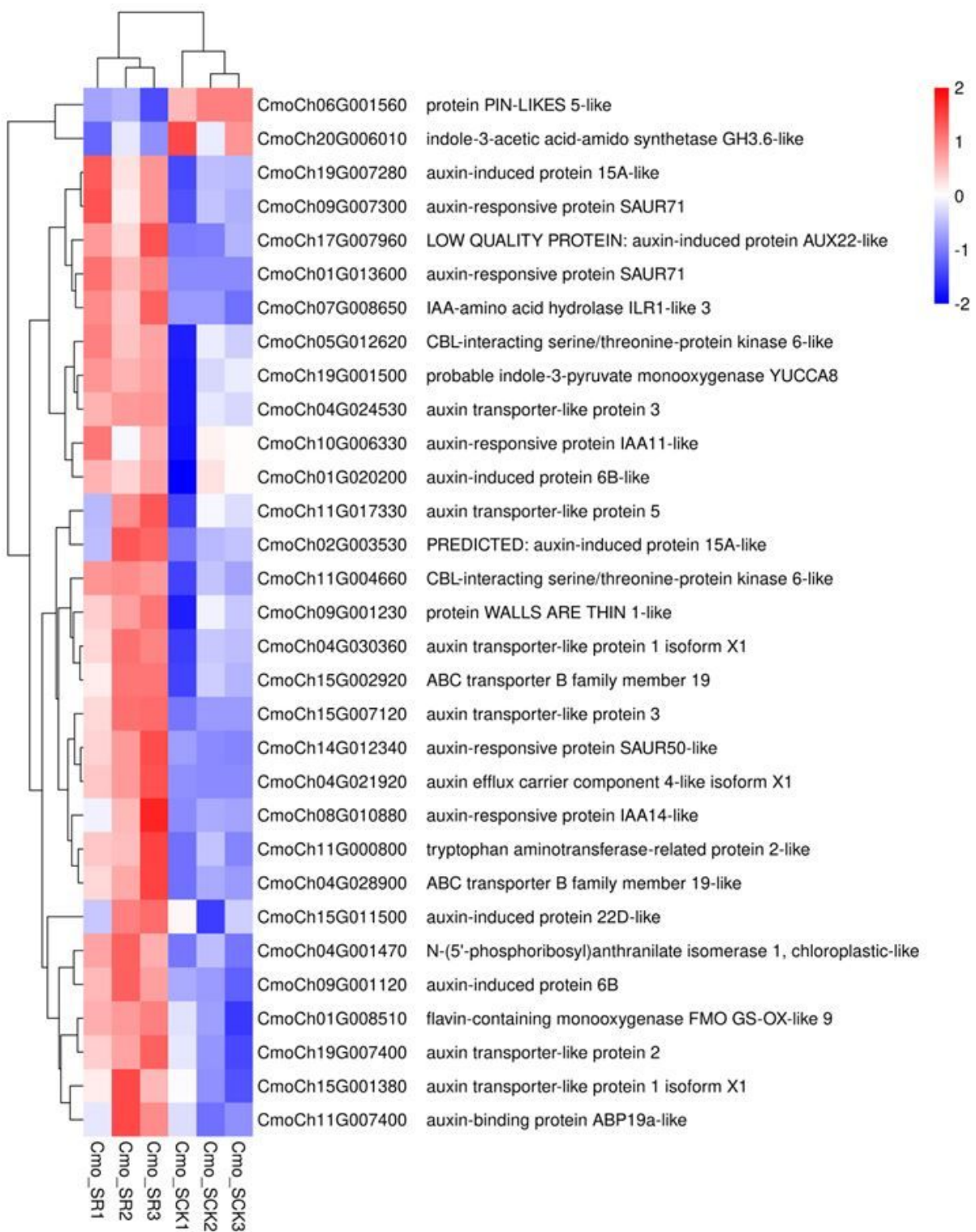


**Figure 5**

Expression heatmap of DEGs related to auxin response in pumpkin during EOD-FR treatment.

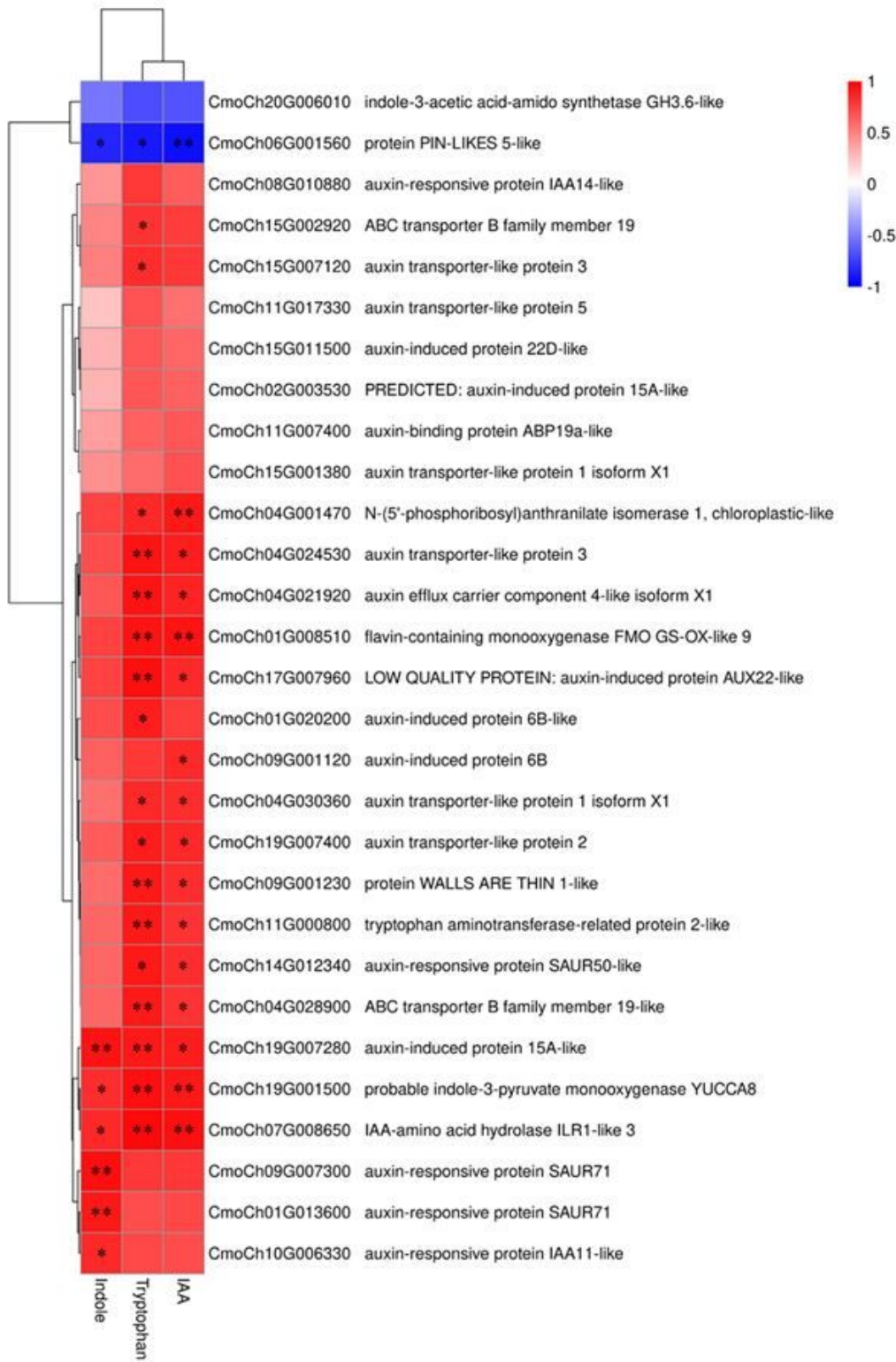


**Figure 6**

Heatmap of correlations between auxin-related DEGs and differentially accumulated auxin metabolites. \* means that the correlation between the two is  $\geq 0.8$ , and \*\* means that the correlation is  $\geq 0.9$ .

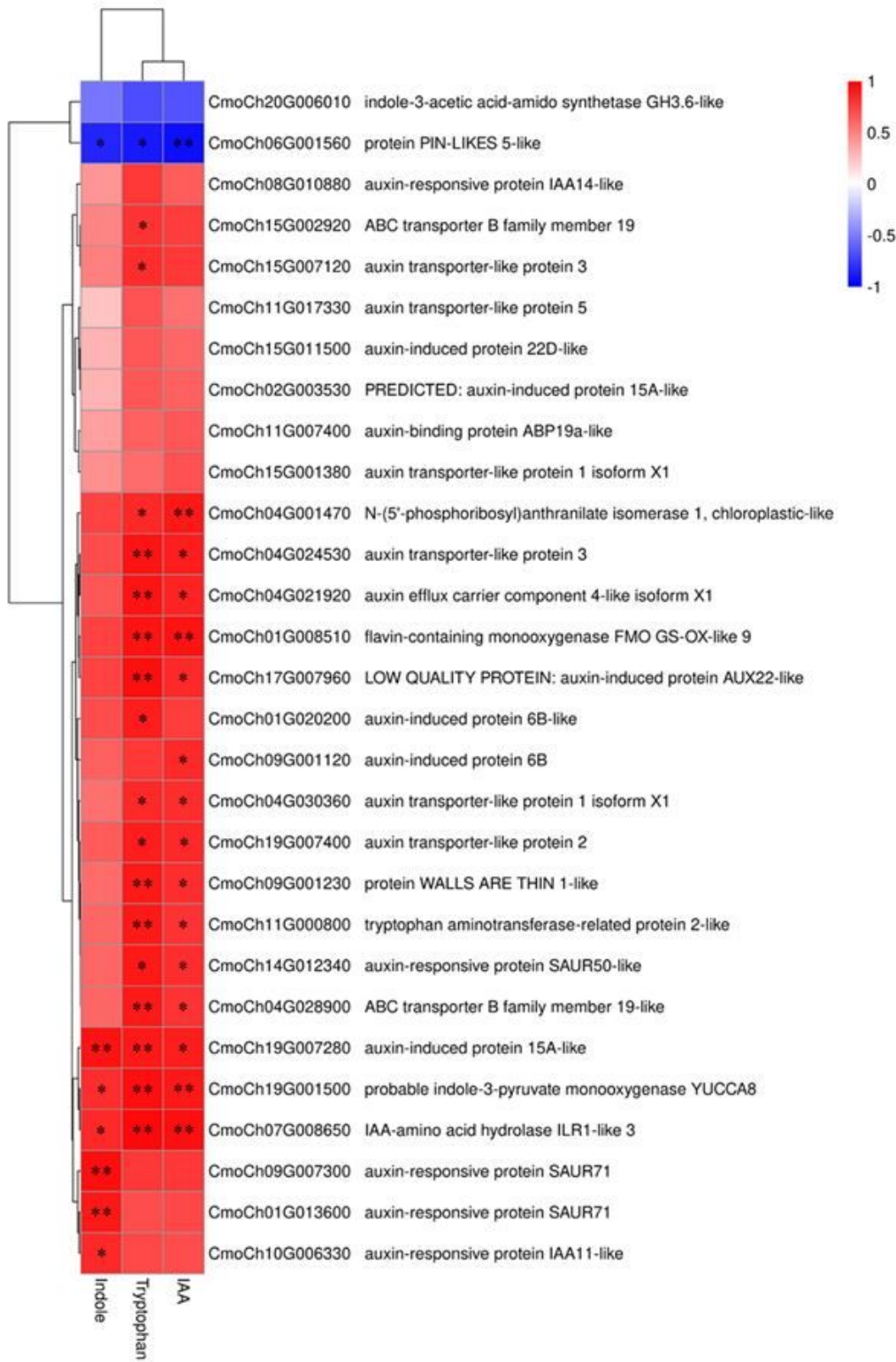


**Figure 6**

Heatmap of correlations between auxin-related DEGs and differentially accumulated auxin metabolites. \* means that the correlation between the two is  $\geq 0.8$ , and \*\* means that the correlation is  $\geq 0.9$ .

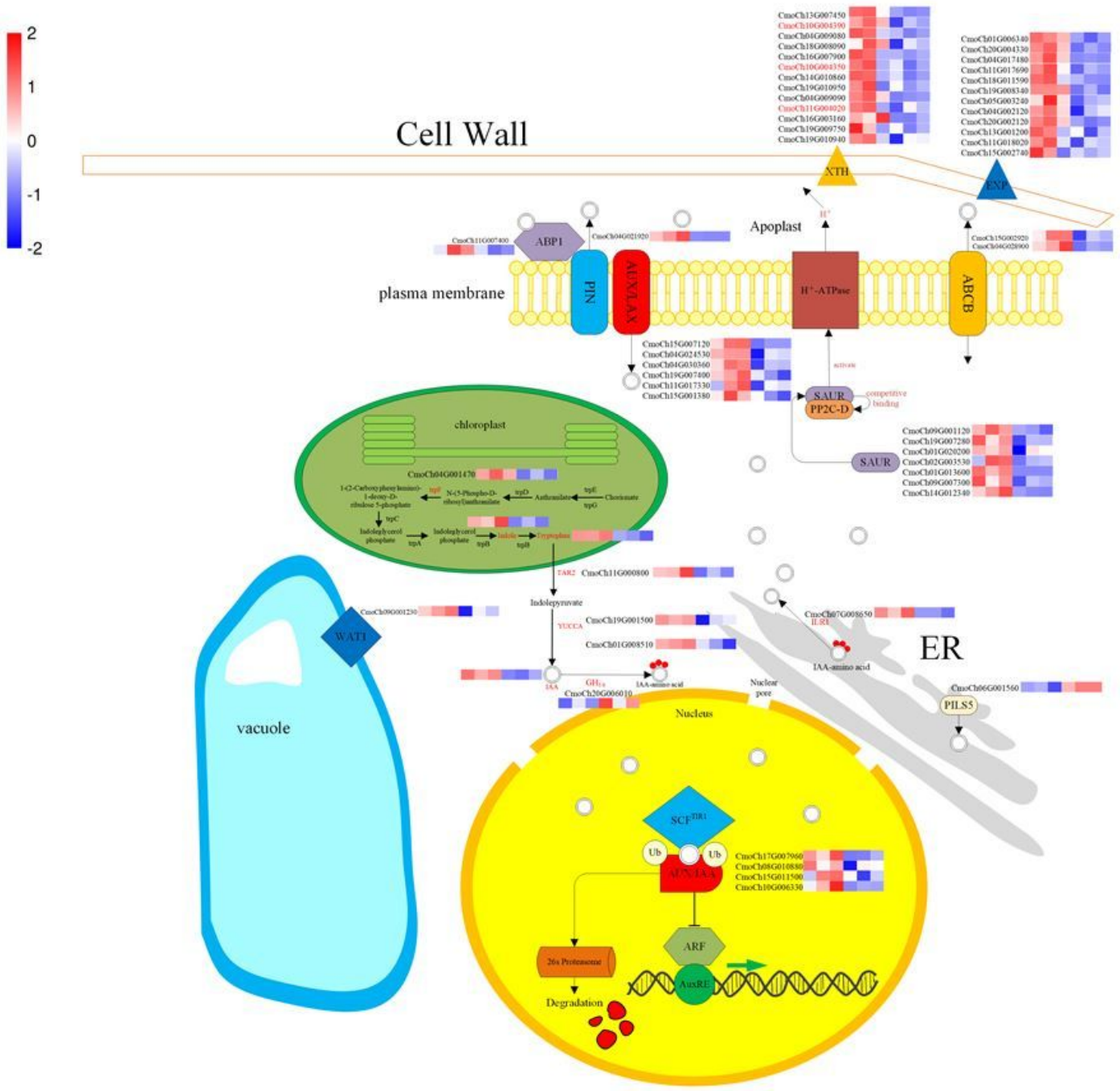


**Figure 7**

Overview of auxin-related metabolism and transcription in pumpkin. During EOD-FR treatment. Different genes and metabolites are represented by different shapes, and the color blocks correspond to log2-transformed FPKM or content data.

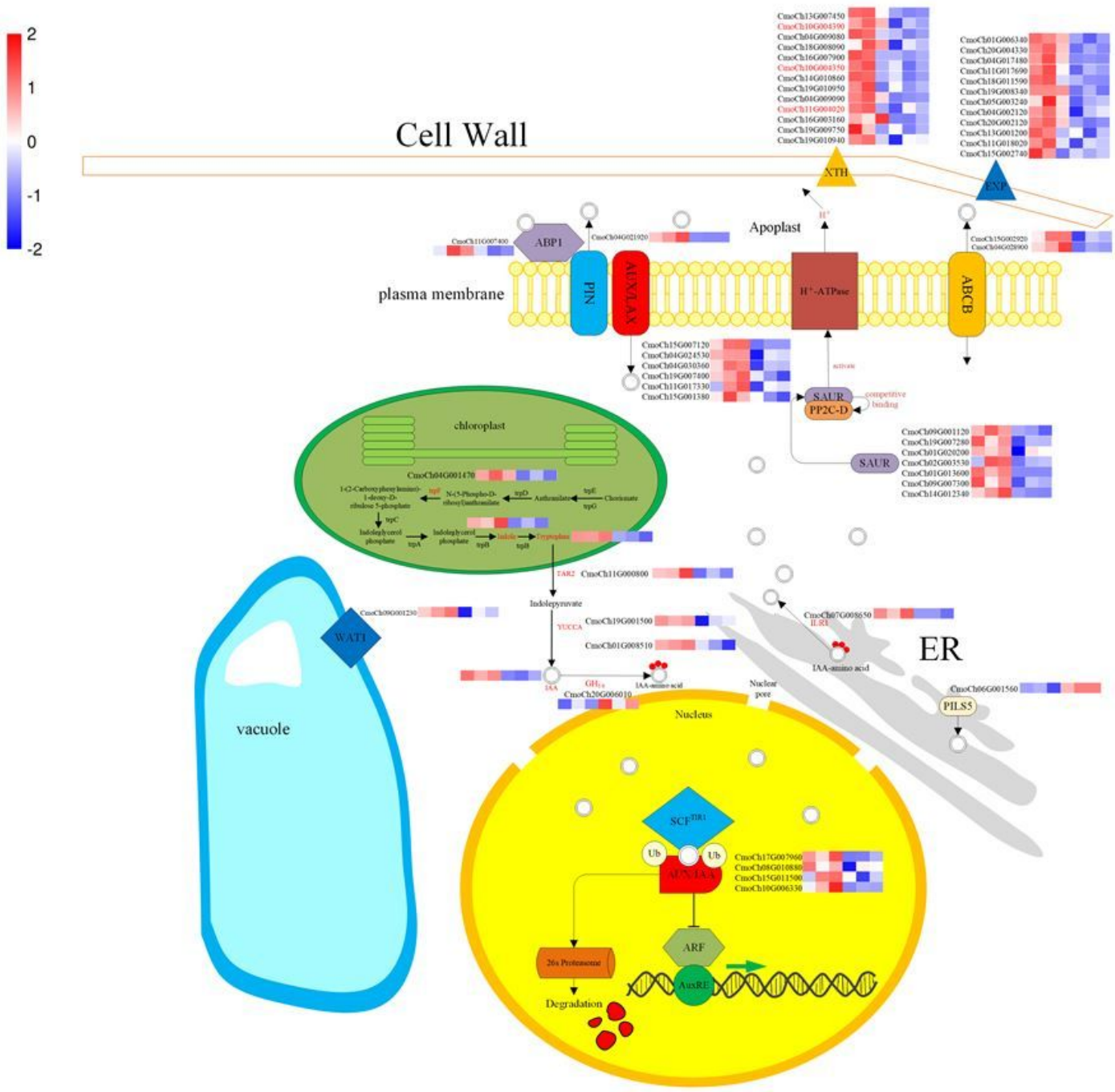


**Figure 7**

Overview of auxin-related metabolism and transcription in pumpkin. During EOD-FR treatment. Different genes and metabolites are represented by different shapes, and the color blocks correspond to log2-transformed FPKM or content data.

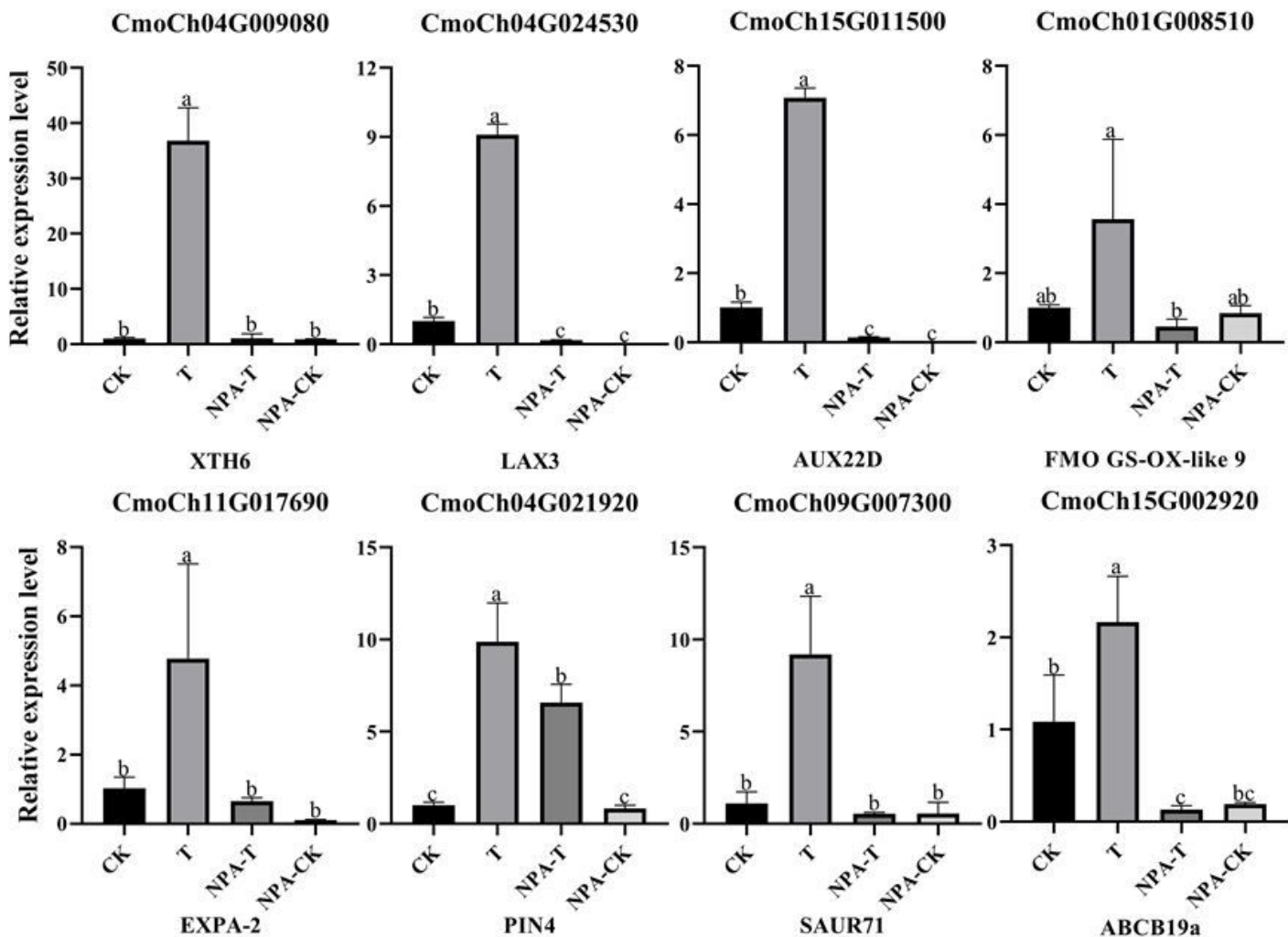


**Figure 8**

Expression of eight genes associated with hypocotyl elongation during EOD-FR treatment. Different lowercase letters between columns indicate a significant difference at the 5% level between treatments; XTH6: probable xyloglucan endotransglucosylase/hydrolase protein 6; LAX3: auxin transporter-like protein 3; AUX22D: auxin-induced protein 22D-like; FMO GS-OX-like 9: flavin-containing monooxygenase FMO GS-OX-like 9; EXPA-2: expansin-like A2; PIN 4: auxin efflux carrier component 4-like isoform X1; SAUR 71: auxin-responsive protein SAUR71; ABCB 19a: ABC transporter B family member 19. Error bars represent  $\pm$ SD.

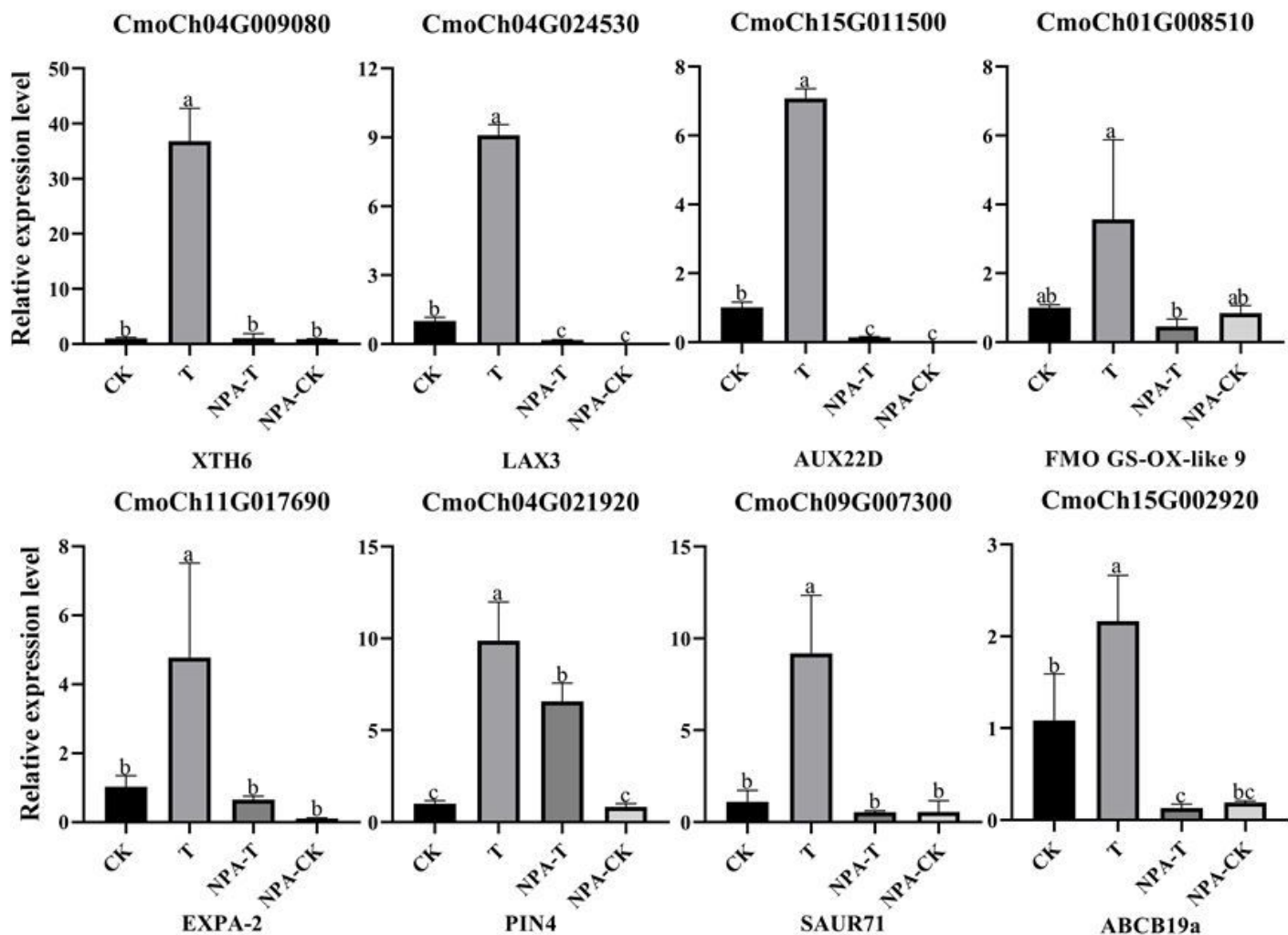


**Figure 8**

Expression of eight genes associated with hypocotyl elongation during EOD-FR treatment. Different lowercase letters between columns indicate a significant difference at the 5% level between treatments; XTH6: probable xyloglucan endotransglucosylase/hydrolase protein 6; LAX3: auxin transporter-like protein 3; AUX22D: auxin-induced protein 22D-like; FMO GS-OX-like 9: flavin-containing monooxygenase FMO GS-OX-like 9; EXPA-2: expansin-like A2; PIN 4: auxin efflux carrier component 4-like isoform X1; SAUR 71: auxin-responsive protein SAUR71; ABCB 19a: ABC transporter B family member 19. Error bars represent  $\pm$ SD.

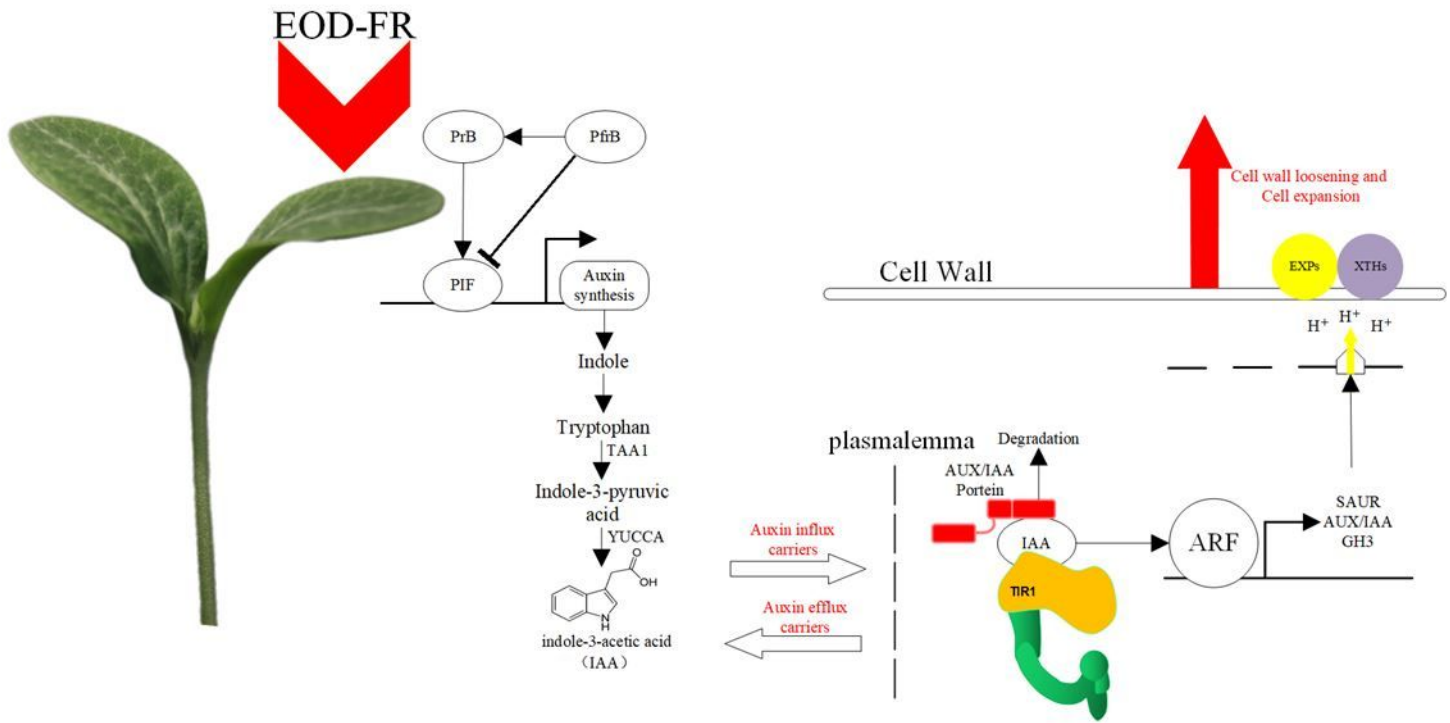


**Figure 9**

A hypothetical diagram summarizing auxin-induced hypocotyl elongation in pumpkin during EOD-FR treatment. The figure depicts several auxin-related biological processes and reactions. Arrows indicate the direction of catalytic reaction or transport. We propose that EOD-FR promotes the conversion of PfrB to PrB, which leads to a decrease in PfrB in the nucleus, thereby relieving the inhibition of PIF. PIF promotes the expression of downstream genes related to auxin synthesis. Based on the experimental data, we conclude that the tryptophan-dependent TAA-YUC pathway is likely to be the main pathway of IAA synthesis induced by EOD-FR. After synthesis, auxin is transported to the hypocotyls by way of the polar auxin transport system and promotes the transcription of downstream auxin response genes. Among them, the products of SAUR genes can promote the activity of H<sup>+</sup>ATPase, leading to apoplast acidification and increased activity of wall proteins such as XTHs and EXPs. This promotes cell expansion and eventually leads to significant hypocotyl elongation.

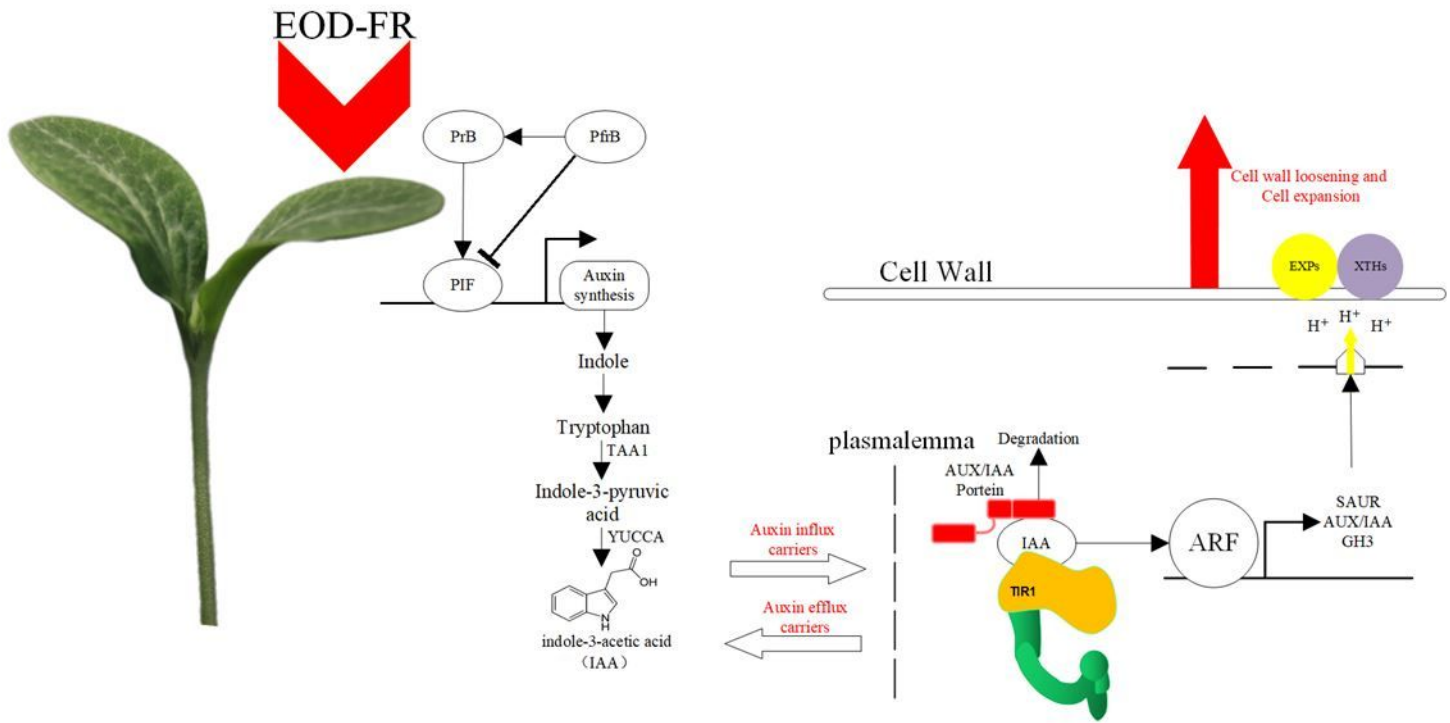


**Figure 9**

A hypothetical diagram summarizing auxin-induced hypocotyl elongation in pumpkin during EOD-FR treatment. The figure depicts several auxin-related biological processes and reactions. Arrows indicate the direction of catalytic reaction or transport. We propose that EOD-FR promotes the conversion of PfrB to PrB, which leads to a decrease in PfrB in the nucleus, thereby relieving the inhibition of PIF. PIF promotes the expression of downstream genes related to auxin synthesis. Based on the experimental data, we conclude that the tryptophan-dependent TAA-YUC pathway is likely to be the main pathway of IAA synthesis induced by EOD-FR. After synthesis, auxin is transported to the hypocotyls by way of the polar auxin transport system and promotes the transcription of downstream auxin response genes. Among them, the products of SAUR genes can promote the activity of H<sup>+</sup>ATPase, leading to apoplast acidification and increased activity of wall proteins such as XTHs and EXPs. This promotes cell expansion and eventually leads to significant hypocotyl elongation.

## Supplementary Files

This is a list of supplementary files associated with this preprint. Click to download.

- [AttacheTable.xls](#)
- [AttacheTable.xls](#)
- [FigS1.tif](#)
- [FigS1.tif](#)
- [FigS5.tif](#)

- FigS5.tif
- Fig.S6.pdf
- Fig.S6.pdf
- FigureS2.tiff
- FigureS2.tiff
- FigureS3.tiff
- FigureS3.tiff
- FigureS4.tiff
- FigureS4.tiff
- FigureS7.tif
- FigureS7.tif
- ListofResponses.doc
- ListofResponses.doc
- Manuscrip11.12.doc
- Manuscrip11.12.doc